

1-1-1964

Spatial dependent transfer function of zero power reactors

Tatsuhiko Tatsuhiko
Iowa State University

Follow this and additional works at: <https://lib.dr.iastate.edu/rtd>



Part of the [Engineering Commons](#)

Recommended Citation

Tatsuhiko, Tatsuhiko, "Spatial dependent transfer function of zero power reactors" (1964). *Retrospective Theses and Dissertations*. 18045.
<https://lib.dr.iastate.edu/rtd/18045>

This Thesis is brought to you for free and open access by the Iowa State University Capstones, Theses and Dissertations at Iowa State University Digital Repository. It has been accepted for inclusion in Retrospective Theses and Dissertations by an authorized administrator of Iowa State University Digital Repository. For more information, please contact digirep@iastate.edu.

SPATIAL DEPENDENT TRANSFER FUNCTION
OF ZERO POWER REACTORS

by

Tatsuhiko Ando

A Thesis Submitted to the
Graduate Faculty in Partial Fulfillment of
The Requirements for the Degree of
MASTER OF SCIENCE

Major Subject: Nuclear Engineering

Signatures have been redacted for privacy

Iowa State University
Of Science and Technology
Ames, Iowa

1964

TABLE OF CONTENTS

	Page
I. INTRODUCTION	1
II. REVIEW OF THE LITERATURE	3
III. THEORETICAL ANALYSIS	7
A. General Form of Transfer Function	7
B. Transfer Functions for Various Geometries	16
IV. NUMERICAL CALCULATION	23
A. Spatial Dependent Transfer Function	23
B. Calculation Method and Core Data	23
C. Results	26
V. DISCUSSIONS	52
A. On the Theory	52
B. On the Results of the Numerical Calculation	55
VI. CONCLUSIONS	59
VII. SUGGESTIONS FOR FURTHER STUDY	61
A. On the Theory	61
B. On the Experiment	62
VIII. NOMENCLATURE	66
IX. BIBLIOGRAPHY	69
X. ACKNOWLEDGMENTS	71
XI. APPENDIX	72

I. INTRODUCTION

A standard method for determining the stability of a nuclear reactor is the transfer function technique, which has been developed in the field of servomechanisms. In control theory the transfer function of a system is defined as the ratio of the Laplace transform of the output to the Laplace transform of the driving function of the system. In order to obtain the transfer function of a system analytically, the differential equation which describes the relation between the input into the system and the output from the system should be solved using the Laplace transformation technique with respect to time.

The physical system of a nuclear reactor is usually treated as a one-point model in which the nuclear reactor is regarded as a point without the spatial extension. Also any physical processes in the reactor are assumed to occur at the same time regardless of the location. This one-point model gives a quite satisfactory approximation to the actual phenomena in the reactor and sufficient information to analyze the stability of the reactor when it is small. Moreover, since the solutions of partial differential equations, which describe the spatial and temporal dependency of the physical processes in the reactor, are of very complicated forms, it is rather troublesome to treat them in control theory. For this reason, the one-point model has been used in the stability analysis of nuclear reactors as a first approximation.

The situation, however, is rather different in the case of large nuclear reactors. It has been found that the spatially independent transfer function causes some error in the high frequency region. With the advancement of more refined nuclear reactor techniques, it has become

necessary to obtain precise information about the effects of the spatial dependence of the phenomena in the core. For example, the oscillator technique is frequently used for the measurement of the transfer function of a reactor and also of reactor parameters. In this case, it is necessary to use a localized neutron absorber and localized neutron detection equipment, because the reactivity cannot be changed uniformly by changing the neutron absorption cross section uniformly over the core. Hence, when the one-point model is used for the analysis, the error introduced by this assumption is unavoidable. Also, most of the inputs or the disturbances to the core, which cause a change in the reactivity, are not spatially uniform over the core. Typical examples of such inputs or disturbances are the movement of control rods, the void generation in a boiling water reactor and Xenon oscillations.

In the present investigation, the spatial dependent transfer function of a zero power nuclear reactor, which does not include the feedback of a temperature coefficient, is obtained in the form of a series expansion of eigen functions. The transfer function is first obtained in the generalized form and it is applied to various core geometries. The transfer functions of two slab type cores are calculated with the aid of the CYCLONE computer and compared with the spatial independent transfer function. Finally the convergence of the series is discussed numerically for this case.

II. REVIEW OF THE LITERATURE

As for the study of the transfer function of the one-point model reactor, much work has been reported (1,4,12,17) and these investigations are summarized in text books (8,18).

In this section the various attempts to treat the spatial and temporal dependence of neutron density in nuclear reactors are reviewed.

The first article which treated the spatial dependence of the change in the neutron density with a localized disturbance was presented by Weinberg and Schweinler (19) in 1948. In this article, it is assumed that the reactor is homogeneous, bare and just critical, the neutron energy group is two and the neutron flux density and the source term of thermal neutrons can be expanded into the series of eigen functions of the Helmholtz equation. The thermal neutron source term is expressed by the integration with the slowing down kernel. The reactor characteristic equation, which is essentially the diffusion equation except for the source term, and the delayed neutron precursor equation, which expresses the time behavior of the delayed neutron generation, are solved with the aid of the Fourier transform for the localized oscillating absorber. This investigation shows that at low frequencies the neutron density rises and falls, always keeping essentially the shape it has before the absorber was oscillated. In turn, at high frequencies the neutron density is depressed locally at the location of the oscillating absorber and this depression in the neutron density is propagated away from the absorber as a damped wave. This result indicates that at high frequencies the magnitude and the phase shift of the reactor transfer function vary with the location of the absorber and the neutron detector. On the other hand, at low

frequencies the relative location of the absorber and the observation does not cause a significant difference in the transfer function. Therefore, the one-point model represents a poor approximation of the actual reactor system for high frequencies.

The eigen function expansion method, in which the solution and coefficients are expanded in an infinite series in sets of expansion function known to be complete, has been investigated by many persons (5,6,11).

Garabedian and Foderaro (5) obtained the series solution for the two energy groups neutron diffusion equations. Each term is expressed as a product of a space-dependent eigen function and a time-dependent factor.

Kaplan (11) proposed the method to expand the solution into the series with the property of finality and succeeded to construct the operator which gives the series the property of finality. The property of finality means that the expansion coefficients are determined by the ordinary differential equations which are independent of the number of terms retained. With this method, the expansion coefficients can be obtained by solving N independent ordinal differential equations ---- N is the number of terms retained ---- while for the general case N dependent differential equations have to be solved simultaneously. This technique simplifies considerably the procedure of the calculation.

An alternative approach to this problem is the variational method (3,13). Although this method has the disadvantage that it is difficult to find the proper trial function and may involve troublesome calculations, it is expected that it will give a new approximation to this problem.

As for the attempts to solve this problem in connection with control theory, Loewe (14,15) solved the two group diffusion equations, the same

one as that of Weinberg and Schweinder, and the delayed neutron precursor equation with the eigen function expansion technique and obtained a transfer function of the matrix form. The result of his numerical calculation shows that the magnitude of the spatial dependent transfer function is larger than that of the spatial independent transfer function and this gap increases with increasing frequency. At low frequencies this gap is not so significant. The phase shift of the spatial dependent transfer function has another peak around $\omega=10^3 \sim 10^4$ rad/sec besides the peak around $\omega=1 \sim 10$ rad/sec, which appears also in the phase shift of spatial independent transfer function. This second peaking in the phase shift does not appear in the theory of the one-point model.

Hayashi, Hoshino and Wakabayashi (9) showed that the Green's function of the diffusion equation under the given boundary condition is the transfer function of the neutron flux to the point neutron source. They solved this problem with the mirror image method for the case of one energy group of the neutron and one delayed neutron group. It has not been clear that this method can be applied to the more general case.

The available experimental work on the space-dependency of the reactor transfer function is that of Hanson and Foulke (7). They measured the transfer function of NORA by the pile oscillator technique for various positions of the neutron detector. They found that the magnitude of the transfer function has the same tendency as that described by Loewe. The phase shift was not measured for frequencies high enough to exhibit a deviation from the space independent case. In order to check their measurement, they simulated the neutron flux response to a localized absorber using an analogue computer. The reactor core was divided into

14 concentric annular regions and the spatial dependency of two group diffusion equations is replaced by difference equations. The temporal dependency of neutron flux in each region is simulated by 14 analogue circuits. They also compared the results of the simulation and the experimental results.

III. THEORETICAL ANALYSIS

A. General Form of Transfer Function

In this section, the general form of the spatial dependent transfer function of a nuclear reactor is derived with the aid of the eigen function expansion method.

The transfer function of a system is defined as the ratio of the Laplace transform of the output from the system to the Laplace transform of the input to the system. It also can be obtained by solving the system of differential equations for an impulse input and taking the Laplace transform of the output, because the Laplace transform of the impulse input becomes a constant.

For the stability analysis of a nuclear reactor, the change in the reactivity and the change in the neutron density are taken as the input and the output of the system, respectively. But the transfer function is defined as the ratio of the Laplace transformed neutron flux change to the Laplace transformed absorption cross section change in this investigation. The reason of this definition is due to the fact that in the actual operation of a reactor and the measurement of the transfer function or other reactor constants the absorption cross section change is mostly used as the input to the nuclear reactor.

The following assumptions are made for the derivation of the transfer function:

1. The reactor is homogeneous and bare.
2. The number of the energy groups of neutron is one.
3. The reactor was in steady state before the input is introduced into

the core.

4. The densities of the delayed neutron precursors as well as the neutron flux vanish at the extrapolated boundary of the core.

The time-dependent neutron flux distribution, $\phi(\vec{r}, t)$, is given as the solution of the diffusion equation:

$$D\nabla^2\phi(\vec{r}, t) - \Sigma_a(\vec{r}, t) + (1 - \beta)\Sigma_{\infty}k_q\phi(\vec{r}, t) + p\sum_{i=1}^M \lambda_i C_i(\vec{r}, t) + S(\vec{r}, t) = \frac{1}{v} \frac{\partial \phi(\vec{r}, t)}{\partial t} \quad 1$$

where

∇^2 = Laplace operator,

\vec{r} = vector to express the position,

D = diffusion coefficient,

Σ_a = absorption cross section of medium,

q = non-leakage factor of the neutron in the slowing down process,

k_{∞} = multiplication factor for the infinite medium,

β = total fraction of delayed neutrons,

p = resonance escape probability,

λ_i = decay constant of the i 'th groups precursor of delayed neutrons,

C_i = concentration of i 'th group precursor of delayed neutrons,

S = extraneous neutron source,

v = average velocity of the thermal neutrons.

The equation for the delayed neutron precursors are given by:

$$\frac{\partial C_i(\vec{r}, t)}{\partial t} = \frac{\beta_i}{\beta} k_{\infty} \Sigma_a \phi(\vec{r}, t) - \lambda_i C_i(\vec{r}, t) \quad 2$$

where β_i = fraction of i 'th group delayed neutrons,
 m - the number of the delayed neutron groups.

If an impulse change of the absorption cross section is introduced into the core at the location \vec{a} at $t=0$, the absorption cross section is expressed as:

$$\Sigma_a = \Sigma_a' - \Delta \Sigma_a \delta(\vec{r}) \delta(t) \quad 3$$

where Σ_a = absorption cross section of the medium,
 Σ_a' = absorption cross section at the steady state
 and constant because of the homogeneity of the
 medium,

δ = Dirac's delta function.

The negative sign is taken because the introduction of a negative change in the absorption cross section causes a positive change in the multiplication factor, k_{∞} . The change, $\delta \Sigma_a$, in the absorption cross section causes a change in the multiplication factor and it is designated δk . Since the multiplication factor, k_{∞} , is defined as:

$$k_{\infty} = \epsilon \eta f \quad 4$$

where ϵ = fast fission factor,

η = average number of neutron produced in the core
 per neutron absorbed, $= \Sigma_{ff} / \Sigma_{af}$,

f = thermal utilization, $= \Sigma_{af} / \Sigma_a$,

Σ_{ff} = fission cross section of the fuel,

Σ_{af} = absorption cross section of the fuel,

and all factors in Equation 4 except f remain constant for the change in the absorption cross section. The new multiplication factor, k'_∞ , becomes

$$k'_\infty = \text{enpf}' = \text{enp} \frac{\Sigma_a f}{\Sigma_a'}$$

The product of the multiplication factor and the absorption cross section remains always constant because

$$k'_\infty \Sigma_a' = (\text{enp} \frac{\Sigma_a f}{\Sigma_a'}) \Sigma_a' = (\text{enp} \frac{\Sigma_a f}{\Sigma_a}) \Sigma_a = k_\infty \Sigma_a$$

Therefore the diffusion equation, Equation 1, becomes

$$\begin{aligned} D \nabla^2 \phi(\vec{r}, t) - (\Sigma_a - \Delta \Sigma_a \delta(\vec{a}) \delta(t)) \phi(\vec{r}, t) + (1 - \beta) \Sigma_a k_\infty q \phi(\vec{r}, t) \\ + \text{pq} \sum_{i=1}^m \lambda_i C_i(\vec{r}, t) = \frac{1}{v} \frac{\partial}{\partial t} \phi(\vec{r}, t). \end{aligned} \quad 5$$

for the case that there is no extraneous neutron source. The neutron flux and the delayed neutron precursor density are separated into the steady state terms and the time dependent terms as

$$\phi(\vec{r}, t) = \phi(\vec{r}, 0) + \phi_u(\vec{r}, t), \quad 6a$$

$$C_i(\vec{r}, t) = C_i(\vec{r}, 0) + C_{iu}(\vec{r}, t), \quad i = 1, 2, \dots, m. \quad 6b$$

The steady state solutions must satisfy the time-independent diffusion equation and precursor equation. Using this requirement for the steady state solutions and neglecting the product of second order term, i.e. the term $\Delta \Sigma_a \phi_u$, the following equations are obtained for the time dependent solutions

$$\begin{aligned} \Delta \nabla^2 \phi_u(\vec{r}, t) - \Sigma_a \phi_u(\vec{r}, t) + \Delta \Sigma_a \delta(\vec{a}) \delta(t) \phi(\vec{r}, 0) \\ + (1-\beta) \Sigma_a k_{\infty} \phi_u(\vec{r}, t) + \rho q \sum_{i=1}^m \lambda_i C_{iu}(\vec{r}, t) = \frac{1}{v} \frac{\partial \phi_u}{\partial t}(\vec{r}, t) \end{aligned} \quad 7$$

and

$$\frac{\partial C_{iu}}{\partial t}(\vec{r}, t) = \frac{\beta_i}{\beta} \Sigma_a k_{\infty} \phi_u(\vec{r}, t) - \lambda_i C_{iu}(\vec{r}, t). \quad 8$$

When the Laplace transformation is applied to Equations 7 and 8, we obtain

$$\begin{aligned} \Delta \nabla^2 \phi(\vec{r}, s) - \Sigma_a \phi(\vec{r}, s) + \Delta \Sigma_a \delta(\vec{a}) \phi(\vec{r}, 0) \\ + (1-\beta) \Sigma_a k_{\infty} \phi(\vec{r}, s) + \rho q \sum_{i=1}^m \lambda_i H_i(\vec{r}, s) = \frac{1}{v} s \phi(\vec{r}, s) \end{aligned} \quad 9$$

and

$$s H_i(\vec{r}, s) = \frac{\beta_i}{\beta} \Sigma_a k_{\infty} \phi(\vec{r}, s) - \lambda_i H_i(\vec{r}, s), \quad i=1, \dots, m. \quad 10$$

where

$$\begin{aligned} \phi(\vec{r}, s) &\equiv \mathcal{L}\{\phi_u(\vec{r}, t)\} \\ H_i(\vec{r}, s) &\equiv \mathcal{L}\{C_{iu}(\vec{r}, t)\}. \end{aligned}$$

The necessary conditions for deriving Equations 9 and 10 are

$$\phi_u(\vec{r}, 0) = 0 \quad \text{and} \quad C_{iu}(\vec{r}, 0) = 0.$$

It is assumed that the solution of Equation 9 can be expanded into the series of eigen functions of the Helmholtz equation

$$\nabla^2 \psi_n(\vec{r}) + B_n^2 \psi_n(\vec{r}) = 0 \quad 11$$

where n represents the vector of the suffix, i.e.,

$n = l\vec{i} + m\vec{j} + n\vec{k}$. ($\vec{i}, \vec{j}, \vec{k}$) is the set of the unit orthogonal vectors, which corresponds to the system coordinate system.

Now consider the integral transform of Equations 9 and 10 with the kernel of an eigen function of Helmholtz equation, $\psi_n(\vec{r})$. The domain of

integration is defined to be the volume of the reactor. Define the integral transformed neutron flux by

$$\varphi(\vec{n}, s) = \int_{\text{core}} \psi_{\vec{n}}(\vec{r}) \phi(\vec{r}, s) d\vec{r} \quad 12$$

and the integral transformed precursor densities by

$$X_1(\vec{n}, s) = \int_{\text{core}} \psi_{\vec{n}}(\vec{r}) H_1(\vec{r}, s) d\vec{r} \quad 13$$

From the assumption of the expansion of the solution, the solution is written as

$$\phi(\vec{r}, s) = \sum_{\vec{n}} A_{\vec{n}}(s) \psi_{\vec{n}}(\vec{r}) . \quad 14$$

Upon multiplying Equation 14 by $\psi_{\vec{n}}(\vec{r})$ and integrating with respect to \vec{r} over the volume of the core, we obtain the following equation from the orthogonality of the eigen functions

$$\int_{\text{core}} \phi(\vec{r}, s) \psi_{\vec{n}}(\vec{r}) d\vec{r} = A_{\vec{n}}(s) \int_{\text{core}} \psi_{\vec{n}}^2(\vec{r}) d\vec{r} , \quad 15$$

therefore the coefficient, $A_{\vec{n}}(s)$, is

$$A_{\vec{n}}(s) = \frac{\int_{\text{core}} \phi(\vec{r}, s) \psi_{\vec{n}}(\vec{r}) d\vec{r}}{\int_{\text{core}} \psi_{\vec{n}}^2(\vec{r}) d\vec{r}} = \frac{\varphi(\vec{n}, s)}{\int_{\text{core}} \psi_{\vec{n}}^2(\vec{r}) d\vec{r}} \quad 16$$

Hence, the Laplace transformed time dependent neutron flux is expressed by

$$\phi(\vec{r}, s) = \sum_{\vec{n}} \frac{\varphi(\vec{n}, s)}{\int_{\text{core}} \psi_{\vec{n}}^2(\vec{r}) d\vec{r}} \psi_{\vec{n}}(\vec{r}) \quad 17$$

Multiplying both sides of Equations 7 and 8 by $\psi_{\vec{n}}(\vec{r})$ and integrating with respect to \vec{r} over the core volume, Equations 9 and 10 become

$$\begin{aligned}
& \int D\psi_{\vec{n}}(\vec{r})\nabla^2\phi(\vec{r},s)d\vec{r} - \int \Sigma_a\psi_{\vec{n}}(\vec{r})\phi(\vec{r},s)d\vec{r} + \int \Delta\Sigma_a\delta(\vec{a})\psi_{\vec{n}}(\vec{r})\phi(\vec{r},0)d\vec{r} \\
& + \int (1-\beta)\Sigma_a k_{\infty}q\psi_{\vec{n}}(\vec{r})\phi(\vec{r},s)d\vec{r} \\
& + \int pq \sum_{i=1}^m \lambda_i \psi_{\vec{n}}(\vec{r})H_i(\vec{r},s)d\vec{r} = \int \frac{1}{v} s\psi_{\vec{n}}(\vec{r})\phi(\vec{r},s)d\vec{r}
\end{aligned}
\tag{18}$$

and

$$\begin{aligned}
\int s\psi_{\vec{n}}(\vec{r})H_i(\vec{r},s)d\vec{r} &= \int \frac{\beta_i}{p} \Sigma_a k_{\infty} \psi_{\vec{n}}(\vec{r})\phi(\vec{r},s)d\vec{r} \\
&- \int \lambda_i \psi_{\vec{n}}(\vec{r})H_i(\vec{r},s)d\vec{r}
\end{aligned}
\tag{19}$$

Since the eigen functions $\psi_{\vec{n}}(\vec{r})$ and the flux $\phi(\vec{r},s)$ are zero at the extrapolated boundary, Green's theorem can be used to rewrite the first term as

$$\begin{aligned}
\int_{\text{core}} D\psi_{\vec{n}}(\vec{r})\nabla^2\phi(\vec{r},s)d\vec{r} &= D \int_{\text{core}} \phi(\vec{r},s)\nabla^2\psi_{\vec{n}}(\vec{r})d\vec{r} \\
&+ D \int_{\text{surface}} (\psi_{\vec{n}}(\vec{r})\nabla\phi(\vec{r},s) - \phi(\vec{r},s)\nabla\psi_{\vec{n}}(\vec{r}))d\vec{r} \\
&= D \int_{\text{core}} \phi(\vec{r},s)\nabla^2\psi_{\vec{n}}(\vec{r})d\vec{r}
\end{aligned}$$

Using the Helmholtz equation, Equation 11, the first term is rewritten as

$$\begin{aligned}
\int_{\text{core}} D\psi_{\vec{n}}(\vec{r})\nabla^2\phi(\vec{r},s)d\vec{r} &= D \int_{\text{core}} \phi(\vec{r},s)\nabla^2\psi_{\vec{n}}(\vec{r})d\vec{r} \\
&= D \int_{\text{core}} \phi(\vec{r},s)(-B_{\vec{n}}^2\psi_{\vec{n}}(\vec{r}))d\vec{r} \\
&= -B_{\vec{n}}^2 D \int_{\text{core}} \phi(\vec{r},s)\psi_{\vec{n}}(\vec{r})d\vec{r} = -B_{\vec{n}}^2 Dv(\vec{n},s)
\end{aligned}
\tag{20}$$

The second term is rewritten as

$$\begin{aligned}
& \int \Delta \Sigma_a(\vec{a}) \psi_{\vec{n}}(\vec{r}) \phi(\vec{r}, 0) d\vec{r} \\
&= \Delta \Sigma_a \int_{\infty} \delta(\vec{a}) \psi_{\vec{n}}(\vec{r}) \phi(\vec{r}, 0) d\vec{r} \\
&= \Delta \Sigma_a \psi_{\vec{n}}(\vec{a}) \phi(\vec{a}, 0)
\end{aligned} \tag{21}$$

because of the property of the Dirac delta function and the fact that the flux $\phi(\vec{r}, s)$ vanishes outside of the core. Then Equations 18 and 19 are written using the integral transformed neutron flux $v(\vec{n}, s)$ and the integral transformed precursor concentrations $X_i(\vec{n}, s)$ as

$$\begin{aligned}
& -D \nabla_{\vec{n}}^2 v(\vec{n}, s) - \Sigma_a v(\vec{n}, s) + \Delta \Sigma_a \psi_{\vec{n}}(\vec{a}) \phi(\vec{a}, 0) \\
& + (1-\beta) \Sigma_a k_{\infty} q v(\vec{n}, s) + \rho q \sum_{i=1}^m \lambda_i X_i(\vec{n}, s) = \frac{1}{v} v(\vec{n}, s)
\end{aligned} \tag{22}$$

and

$$s X_i(\vec{n}, s) = \frac{\beta_i}{p} \Sigma_a k_{\infty} q v(\vec{n}, s) - \lambda_i X_i(\vec{n}, s), \quad i=1, 2, \dots, m, \tag{23}$$

When Equations 22 and 23 are solved formally for $v(\vec{n}, s)$ and $X_i(\vec{n}, s)$, the solutions become

$$\begin{aligned}
v(\vec{n}, s) = & \frac{\Delta \Sigma_a \phi(\vec{a}, 0) \psi_{\vec{n}}(\vec{a})}{\frac{s}{v} + D \nabla_{\vec{n}}^2 + \Sigma_a - (1-\beta) \Sigma_a k_{\infty} q - \Sigma_a k_{\infty} q \sum_{i=1}^m \frac{\lambda_i \beta_i}{s + \lambda_i}}
\end{aligned} \tag{24}$$

and

$$X_i(\vec{n}, s) = \frac{1}{s + \lambda_i} \frac{\beta_i}{p} \Sigma_a k_{\infty} q v(\vec{n}, s), \quad i=1, 2, \dots, m. \tag{25}$$

Therefore, from Equations 17 and 24, the Laplace transformed neutron flux response to the localized impulse absorption cross section change is obtained as

$$\phi(\vec{r}, s) = \frac{\int \frac{\psi_{\vec{n}}(\vec{r})}{\psi_{\vec{n}}^2(\vec{r})} d\vec{r}}{\frac{s}{v} + DB_{\vec{n}}^2 + \Sigma_a - (1-\beta)\Sigma_a k_{\infty} - \Sigma_a k_{\infty} \sum_{i=1}^{\infty} \frac{\lambda_i \beta_i}{s + \lambda_i}} \frac{\Delta \Sigma_a \phi(\vec{a}, 0) \psi_{\vec{n}}(\vec{a})}{26}$$

Since this solution is the response to the impulse input of magnitude $\Delta \Sigma_a$, the space dependent transfer function, of which the input is the localized absorption cross section change, becomes as

$$\begin{aligned} Q(\vec{r}, s) &= \frac{\phi(\vec{r}, s)}{\mathcal{L}\{\Sigma_a(\vec{a}, s)\}} \\ &= \phi(\vec{a}, 0) \frac{\int \frac{\psi_{\vec{n}}(\vec{r})}{\psi_{\vec{n}}^2(\vec{r})} d\vec{r}}{\frac{s}{v} + DB_{\vec{n}}^2 + \Sigma_a - (1-\beta)\Sigma_a k_{\infty} - \Sigma_a k_{\infty} \sum_{i=1}^{\infty} \frac{\lambda_i \beta_i}{s + \lambda_i}} \\ &\quad \times \frac{\psi_{\vec{n}}(\vec{a})}{27} \end{aligned}$$

It can be proved that the formal solution, Equation 27, actually satisfies Equations 7 and 8 by applying the inverse Laplace transformation to Equation 27 and 25 and substituting into Equations 7 and 8.

It is also easily shown that the first term of Equation 27 is the transfer function of the one-point model. In the case of the one-model, since the spatial distribution is neglected, the terms which are functions of the positions of the absorber and the observation become constant. Also in the process of the derivation of the one-point model transfer function, the spatial dependent term in the diffusion equation, $\nabla^2 \phi$, is replaced by the $B^2 \phi$, in which B^2 is the fundamental eigen value of the Helmholtz equation. This fact indicates that the fundamental term in

Equation 27 is taken into consideration. Then defining the effective neutron life time by

$$l^* = \frac{l}{1 + L^2 B_0^2} = \frac{1}{(1 + L^2 B_0^2) v \Sigma_a}$$

where L is the diffusion length, and putting

$$\frac{k_{\infty} \rho}{1 + L^2 B_0^2} = k_{\text{eff}} = 1,$$

the first term of Equation 27 is easily shown to have the form of

$$\frac{k(s+\lambda)}{l^* s(s+\lambda+B/l^*)}$$

for the one group delayed neutron case.

B. Transfer Functions for Various Geometries

In this section, the actual spatial dependent transfer functions for various fundamental geometries of the core are calculated. Selected geometries of core are the rectangular, the infinite cylinder and the sphere.

1. Rectangular core

In the rectangular coordinates system, the Laplacian is

$$\nabla^2 = \frac{\partial^2}{\partial x^2} + \frac{\partial^2}{\partial y^2} + \frac{\partial^2}{\partial z^2}.$$

The eigen functions which satisfy the Helmholtz equation are the cosine series and the sine series. The eigen functions which satisfy the boundary condition,

$$\psi_n = 0 \text{ at } \vec{r} = (x,y,z) = (0,0,0) \text{ and } \vec{r} = (a,b,c),$$

is only the sine series. Therefore

$$\psi_n(x,y,z) = \sin \frac{l\pi}{a} x \sin \frac{m\pi}{b} y \sin \frac{n\pi}{c} z \quad 28$$

where (a,b,c) is the dimensions of the core in the (x,y,z) directions.

The coefficient of expansion, $\int_{\text{core}} \psi_n^2(\vec{r}) d\vec{r}$, is calculated to be

$$\begin{aligned} \int_{\text{core}} \psi_n^2(\vec{r}) d\vec{r} &= \int_0^a \int_0^b \int_0^c \sin^2 \frac{l\pi}{a} x \sin^2 \frac{m\pi}{b} y \sin^2 \frac{n\pi}{c} z \, dx \, dy \, dz \\ &= \frac{abc}{8} \end{aligned} \quad 29$$

Therefore, the spatial dependent transfer function is given for the rectangular core as

$$\begin{aligned} G(x,y,z;s) &= \frac{8}{abc} \sin \frac{\pi}{a} \alpha_x \sin \frac{\pi}{b} \alpha_y \sin \frac{\pi}{c} \alpha_z \\ &\sum_{l,m,n=1}^{\infty} \frac{\sin \frac{l\pi}{a} \alpha_x \sin \frac{m\pi}{b} \alpha_y \sin \frac{n\pi}{c} \alpha_z \sin \frac{l\pi}{a} x \sin \frac{m\pi}{b} y \sin \frac{n\pi}{c} z}{\frac{8}{v} + DBn^2 + \{ \sum_a - (1-\beta) \sum_a k_{\infty} q \} - \sum_a k_{\infty} q \sum_{i=1}^j \frac{\lambda_i \beta_i}{s+\lambda_i}} \end{aligned} \quad 30$$

where

$$B_n^2 = \left(\frac{l\pi}{a}\right)^2 + \left(\frac{m\pi}{b}\right)^2 + \left(\frac{n\pi}{c}\right)^2.$$

Since the steady state flux distribution $\phi(\vec{r},0)$ is the fundamental mode of eigen functions,

$$\phi(\vec{a},0) = \sin \frac{\pi}{a} \alpha_x \sin \frac{\pi}{b} \alpha_y \sin \frac{\pi}{c} \alpha_z$$

where $(\alpha_x, \alpha_y, \alpha_z)$ is the location of the absorber.

2. Infinite cylindrical core

Since the solution for the finite cylindrical core is obtained by the superposition of the solution for the infinite cylindrical core and the solution for the slab core, the solution for the infinite cylindrical

core is obtained in this section.

The Helmholtz equation in the cylindrical coordinates system is written as

$$\frac{1}{r} \frac{\partial}{\partial r} \left(r \frac{\partial \psi_n}{\partial r} \right) + \frac{1}{r^2} \frac{\partial^2 \psi_n}{\partial \varphi^2} + k_n^2 \psi_n = 0 \quad 31$$

The φ component of the solution of Equation 31 is the linear combination of $\cos l\varphi$ and $\sin l\varphi$. The r component is the linear combination of $J_l(kr)$ and $Y_l(kr)$, where J_l and Y_l are the first and the second kind Bessel functions, respectively.

For simplicity of the calculation, the coordinate system is chosen so that $\alpha_\varphi = 0$, i.e., the location of the absorber is $(r, \varphi) = (ar, 0)$.

From the requirement of the periodicity of the solution, the l must be integers. For the symmetry of the effect of the localized absorber, the φ component of the solution is $\cos l\varphi$.

Since the solution is finite over the core and $Y_l(r)$ has a singularity at $r = 0$, the r component of the solution is represented by $J_l(kr)$.

From the boundary condition, $\psi_n = 0$ at $r = R$, k becomes

$$k = \frac{a_{l,m}}{R} = B_{l,m}$$

where $a_{l,m}$ is the m the zero of $J_l(z)$.

Therefore the eigen function which is used for the expansion of the solution is

$$\psi_n = \cos l\varphi J_l\left(\frac{J_{l,m}}{R} r\right) \quad 32$$

When we calculate the coefficient of the expansion, we obtain

$$\int \psi_n^2(\vec{r}) d\vec{r} = \int_0^{2\pi} d\varphi \int_0^R \cos^2 l\varphi J_l^2\left(\frac{J_{l,m}}{R} r\right) r dr = \frac{\pi R^2}{2} J_{l+1}^2(J_{l,m}) \quad 33$$

also,

$$\phi(\vec{a}, 0) = \phi(a_r, 0; 0) = J_0\left(\frac{j_{0,0}}{R} a_r\right).$$

Therefore, the spatial dependent transfer function of an infinite cylindrical core is

$$G(r, \varphi; s) = \frac{2}{\pi R^2} J_0\left(\frac{j_{0,0}}{R} a_r\right) \times \sum_{l,m=0}^{\infty} \frac{J_l(B_{l,m} a_r)}{J_{l+1}(B_{l,m} R)} \times \frac{\cos l \varphi \cdot J_l(B_{l,m} r)}{\frac{s}{v} + DB_{l,m}^2 + \{\Sigma_a - (1-\beta)\Sigma_a k_{\infty} q\} - \Sigma_a k_{\infty} q \sum_{i=1}^J \frac{\lambda_i \beta_i}{s + \lambda_i}} \quad 34$$

where

$(a_r, 0)$ = position of the localized absorber,

(r, φ) = position of the observation,

$$B_{l,m}^2 = \left(\frac{j_{l,m}}{R}\right)^2$$

3. Spherical core

The Helmholtz equation for the spherical coordinates system is written

as

$$\frac{1}{r^2} \frac{\partial}{\partial r} \left(r^2 \frac{\partial \psi_{\vec{n}}}{\partial r} \right) + \frac{1}{r^2 \sin \theta} \frac{\partial}{\partial \theta} \left(\sin \theta \frac{\partial \psi_{\vec{n}}}{\partial \theta} \right) + \frac{1}{r^2 \sin^2 \theta} \frac{\partial^2 \psi_{\vec{n}}}{\partial \varphi^2} + B_{\vec{n}}^2 \psi_{\vec{n}} = 0 \quad 35$$

The r -, θ - and φ - components of the solution of Equation 34 are the linear combination of followings:

$$\text{r-component } \sqrt{\frac{1}{kr}} J_{n+\frac{1}{2}}(kr) \quad \text{and} \quad \sqrt{\frac{1}{kr}} Y_{n+\frac{1}{2}}(kr)$$

$$\theta\text{-component } P_n^m(\cos\theta) \quad \text{and} \quad Q_n^m(\cos\theta)$$

$$\varphi\text{-component } \cos m\varphi \quad \text{and} \quad \sin m\varphi.$$

where

$J_{n+\frac{1}{2}}$ and $Q_{n+\frac{1}{2}}$ are half order Bessel functions of the first kind and of the second kind, respectively

P_n^m and Q_n^m are associated Legendre functions of the first kind and of the second kind, respectively.

When the coordinates system is picked in such a way that the position of the absorber is

$$\vec{a} = (a_r, a_\theta, a_\varphi) = (a_r, 0, 0),$$

then from the requirement of periodicity and the symmetry of the solution as in the case of the infinite cylindrical core, m becomes integer and the sine series in the φ -component of the solution is discarded. Also, since the solution is finite over the core region and Y_n and Q_n^m have singularities at $r = 0$ and $\theta = 0$, respectively, Y_n and Q_n^m are discarded. From the boundary condition, $\psi_n = 0$ at $r = R$, k is obtained as

$$k = \frac{j_{n,l}}{R} = B_{n,l}$$

where $j_{n,l}$ is the l th zero of $J_{n+\frac{1}{2}}(z)$.

Therefore the eigen functions for the expansion of the solution are

$$\psi_n = \cos m\varphi P_n^m(\cos\theta) \frac{1}{B_{n,l} r} J_{n+\frac{1}{2}}(B_{n,l} r) \quad 36$$

$$n, l = 1, 2, \dots$$

$$m = 1, 2, \dots, n.$$

The coefficient, $\int \psi_{\vec{n}}^2 d\vec{r}$, of the expansion becomes

$$\int \psi_{\vec{n}}(\vec{r})^2 d\vec{r} = \int_0^{2\pi} d\varphi \int_0^{\pi} \sin\theta d\theta \int_0^R r^2 dr \cos n\varphi P_n^m(\cos\theta) \frac{1}{B_{n,l}} J_{n+\frac{1}{2}}(B_{n,l}r) .$$

When the integrations of each components are performed, the following results are obtained

$$\int_0^{2\pi} \cos^2 n\varphi d\varphi = \pi$$

$$\int_0^{\pi} \sin\theta \{P_n^m(\cos\theta)\}^2 d\theta = \int_{-1}^1 \{P_n^m(x)\}^2 dx = \frac{2(n+m)!}{(2n+1)(n-m)!}$$

$$\begin{aligned} \int_0^R \frac{r}{B_{n,l}} J_{n+\frac{1}{2}}(B_{n,l}r)^2 dr &= \frac{\pi R^2}{2B_{n,l}} J_{n+\frac{3}{2}}(B_{n,l}R)^2 \\ &= \frac{\pi R^2}{2J_{n,l}} J_{n+\frac{3}{2}}(J_{n,l})^2 \end{aligned}$$

Therefore

$$\int \psi_{\vec{n}}^2(\vec{r}) d\vec{r} = \frac{(n+m)!}{(n+m)(n-m)!} \frac{\pi R^2}{J_{n,l}} J_{n+\frac{3}{2}}(J_{n,l})^2, m < n \quad 37$$

Since the location of the localized absorber is chosen as $\vec{a} = (a_r, 0, 0)$

and $P_0^0(\cos 0) = 1$ and $\cos(m\theta) = 1$, $\phi(\vec{a}, 0)$ becomes

$$\phi(\vec{a}, 0) = \frac{1}{B_{\infty a_r}} J_{\frac{1}{2}}(B_{\infty a_r}) = \left(\frac{2}{\pi}\right)^{\frac{1}{2}} \frac{\sin(B_{\infty a_r})}{B_{\infty a_r}}$$

Therefore, the spatial dependent transfer function of the spherical core is

$$O(r, \theta, \varphi; s) = \frac{1}{2^{\frac{1}{2}}} \frac{\sin(B_{\infty} a_r)}{B_{\infty} a_r}$$

$$\times \sum_{n=1}^{\infty} \frac{J_{n,l} J_{n+\frac{1}{2}}(B_{n,l} a_r)}{J_{n+\frac{3}{2}}(j_{n,l})^2} \cos \varphi P_n^m(\cos \theta) \frac{1}{B_{n,l} r} J_{n+\frac{1}{2}}(B_{n,l} r)$$

$$\times \frac{\frac{s}{v} + DB_{n,l}^2 + \{\epsilon_a - (1-\beta)\epsilon_a k_{\infty} q\} - \epsilon_a k_{\infty} q}{i=1} \sum_{i=1}^j \frac{\lambda_i s_i}{s + \lambda_i}$$

38

where

$$B_{n,l}^2 = \left(\frac{j_{n,l}}{R} \right)^2$$

$j_{n,l}$ = the l th zero of $J_{n+\frac{1}{2}}(z)$.

IV. NUMERICAL CALCULATION

A. Spatial Dependent Transfer Function

The spatial dependent transfer function can be derived by the method described in III. B. for the core of slab geometry. For simplicity of the calculation, it is assumed that the number of delayed neutron groups is one.

The eigen functions of the one dimensional Helmholtz equation are the sine series and the cosine series. Only the sine series satisfies the boundary condition, $\psi_n = 0$ at $x = 0$ and $x = a$. The eigen values are found to be $(n\pi/a)$, $n = 1, 2, \dots$. Hence, the transfer function is

$$G(x,s) = \frac{2}{a} \sin \frac{n\pi}{a} \sum_{n=1}^{\infty} \frac{v(s+\lambda)}{s^2 + E_n + F_n} \sin \frac{n\pi}{a} \sin \frac{n\pi}{a} x,$$

where

$$E_n = (D(\frac{n\pi}{a})^2 + \Sigma_a - (1-\beta) \Sigma_a k_{\infty} q) v + \lambda$$

$$F_n = (E_n - \lambda - \beta \Sigma_a k_{\infty} q v) \lambda.$$

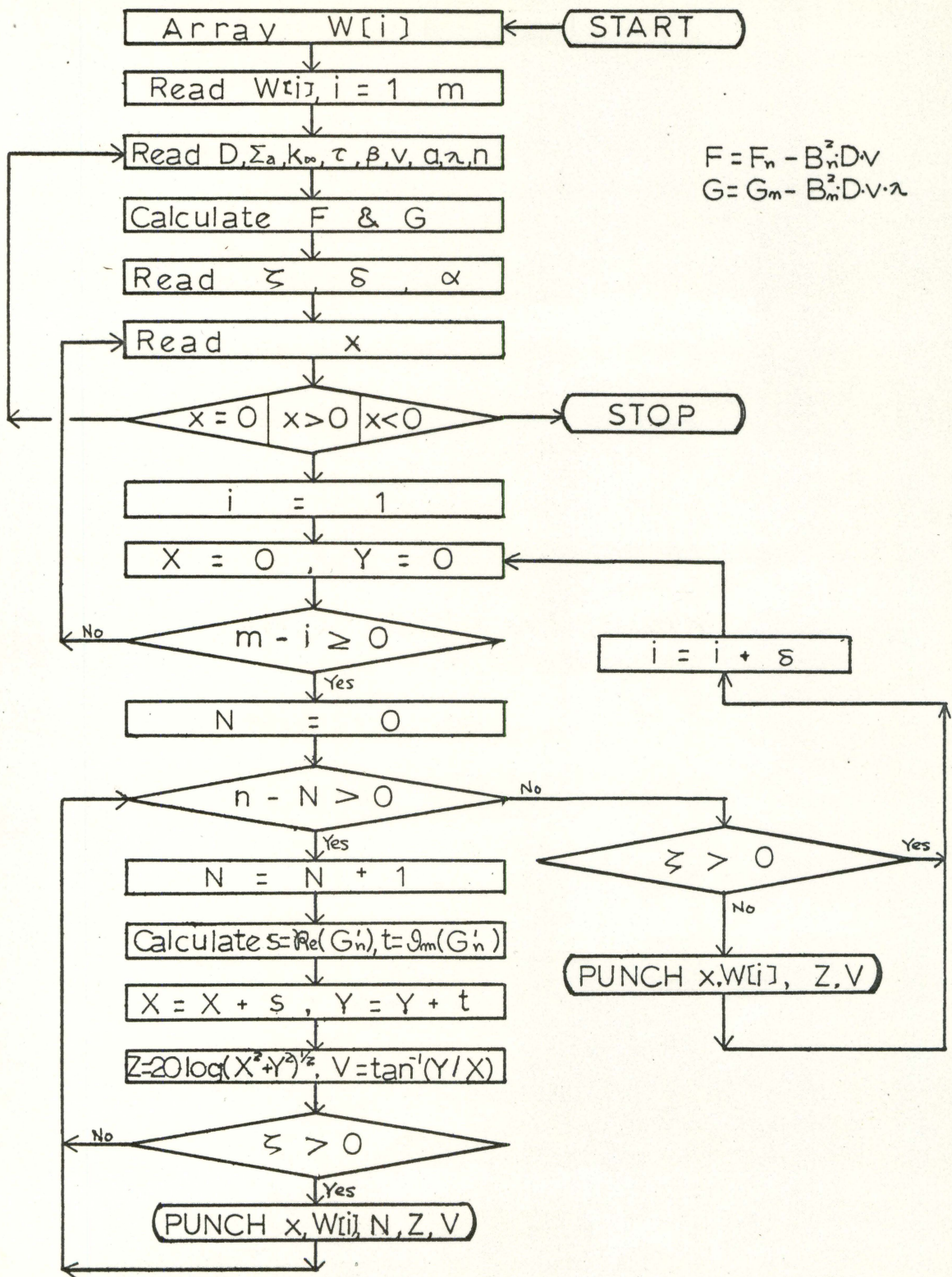
Since the constant term outside of the summation results in a vertical movement of the magnitude in the Bode diagram, the calculation is performed in the following form

$$\frac{G(x,s)}{\frac{2v \sin \frac{n\pi}{a}}{a \sin \frac{n\pi}{a}}} = \sum_{n=1}^{\infty} \frac{s + \lambda}{s^2 + E_n + F_n} \sin \frac{n\pi}{a} \sin \frac{n\pi}{a} x.$$

B. Calculation Method and Core Data

The calculation of the series is performed with the aid of the CYCLONE computer of Iowa State University of Science and Technology. Figure 1 shows the flow chart of the calculation.

Figure 1. Flow chart of calculation



Two reactors are examined in this calculation. One is a natural uranium, heavy water moderated reactor and has a large diffusion length and Fermi age (10). The other is a fully enriched uranium, light water moderated reactor with a small diffusion length and Fermi age. The second reactor composition appears often in the swimming pool type of reactor. The core data and the calculation parameters are tabulated in Table 1.

C. Results

Since the total number of the calculated data amounts to 1155 cases, only typical results, which will reveal the special feature of this theory, are to be represented here.

Figure 2 and Figure 3 show the magnitude, $|G|$, and the phase shift, $\angle G$, respectively, of Reactor I and Reactor II. Figure 4 and Figure 5 show the convergence tendency of the series. These four figures illustrate the results for the case in which the locations of the localized absorber and the observation are same.

From Figure 6 to Figure 13 the magnitude and the phase shift are shown and the convergence tendency of the series for the case in which the neutron flux fluctuation is observed at several locations apart from the location of the oscillating absorber.

Some of the calculated values which are shown in Figure 2 to Figure 5 are tabulated in the Appendix.

Table 1. Core data and calculation parameters¹⁾

		Reactor I	Reactor II
Type		Natural uranium Heavy water moderated	Fully enriched uranium Light water moderated
k_{∞}		1.177	1.600
D	cm	0.82	0.2712
Σ_a	cm ⁻¹	0.0046	0.09235
L^2	cm ²	197	2.958
τ	cm ²	107	42
$a^{2)}$	cm	130	30
ω	rad/sec	(1.0, 1.6, 2.5, 4.0, 6.4,) $\times 10^{-1} \sim 10^5$	
α	cm	60	15
x	cm	65, 60, 50, 35, 20, 5	15, 10, 7, 4, 1,
n		10	

1) The common parameters for both reactors are

$$\beta = 0.0064$$

$$\lambda = 0.08.$$

2) The critical dimension, a, is picked to keep the reactor just critical.

Figure 2. Magnitude vs frequency for Reactor I and Reactor II, same positions of absorber and neutron detector

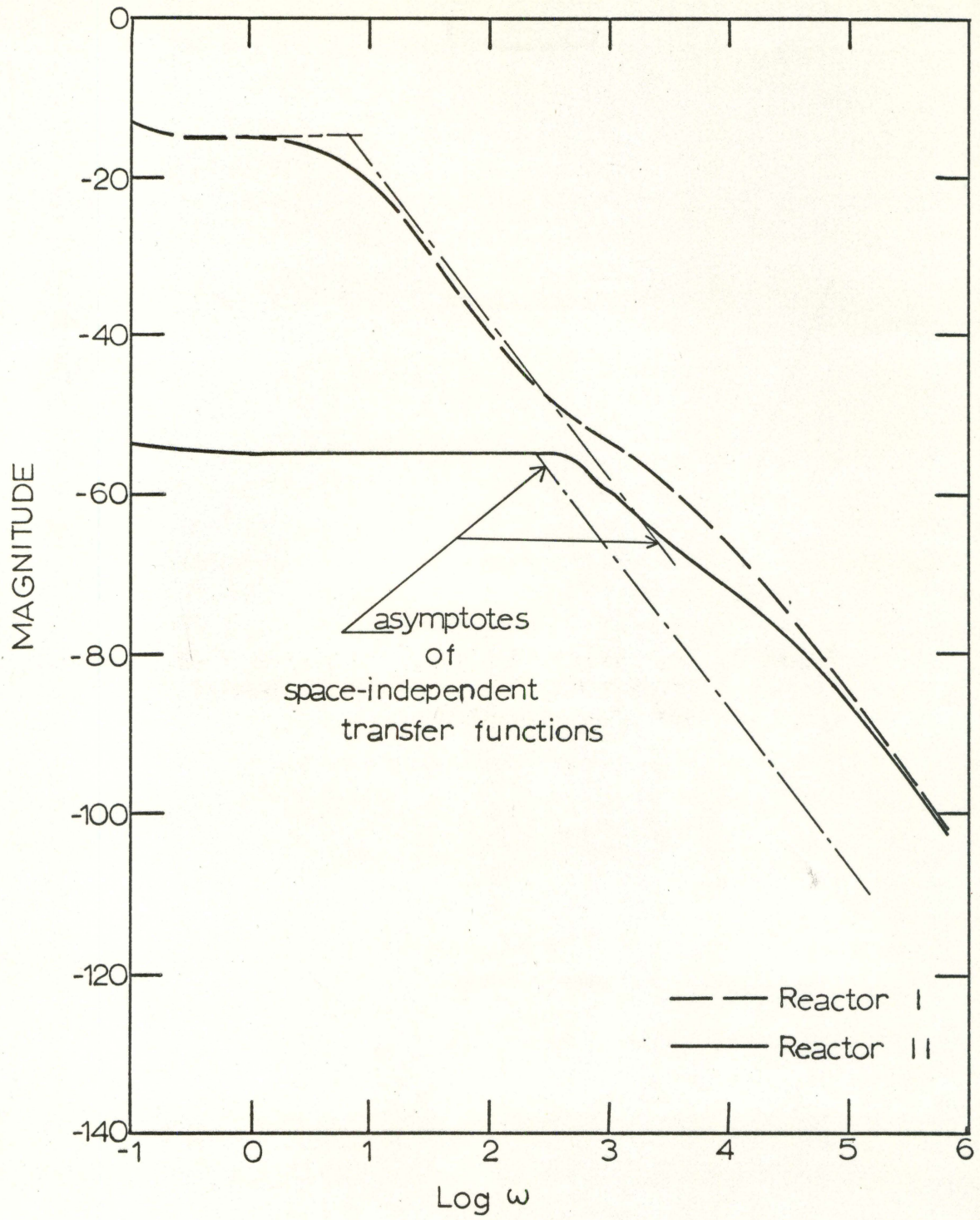


Figure 3. Phase shift vs frequency for Reactor I and Reactor II, same positions of absorber and neutron detector

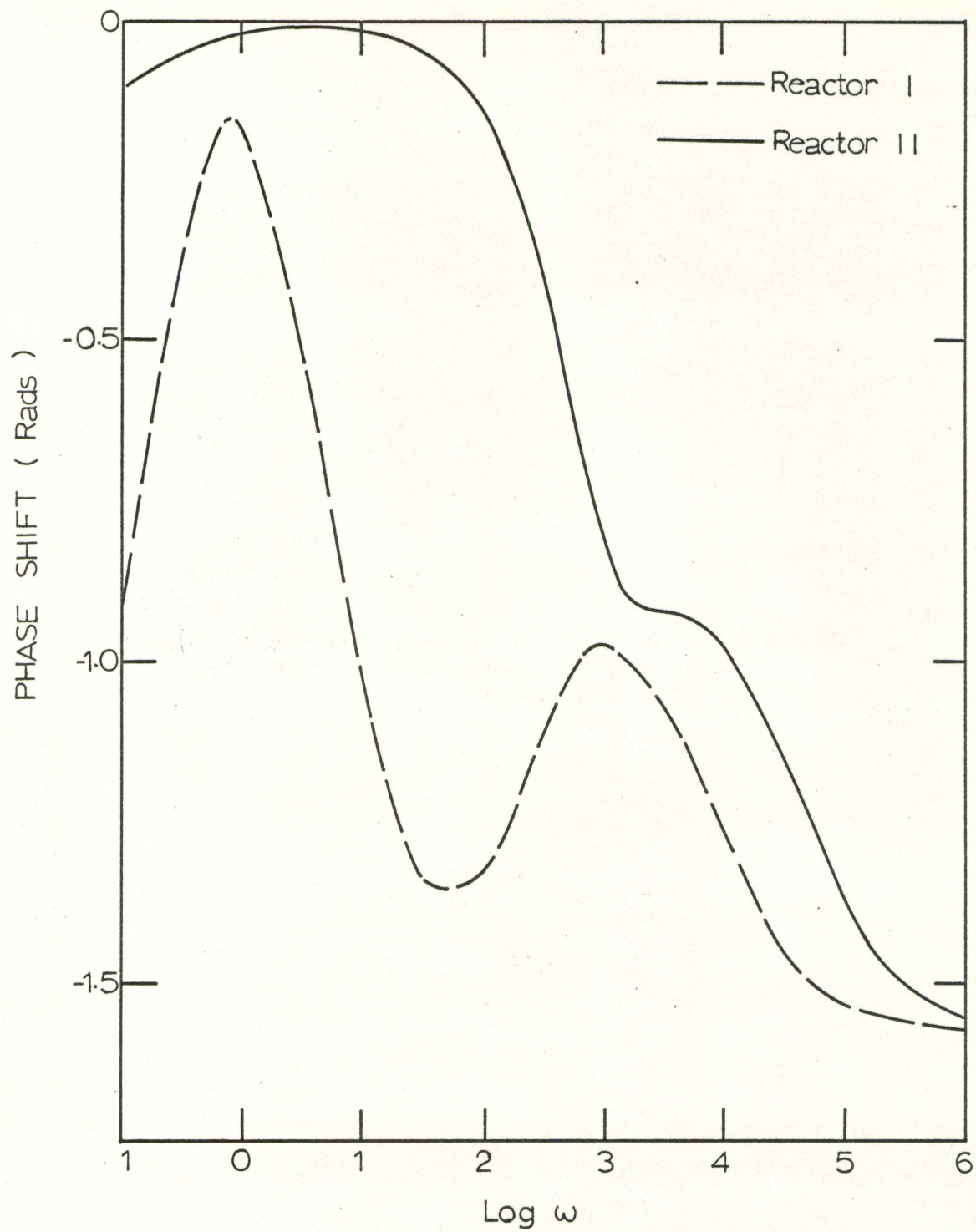


Figure 4. Magnitude vs number of terms for Reactor I
and Reactor II, same positions of absorber
and neutron detector

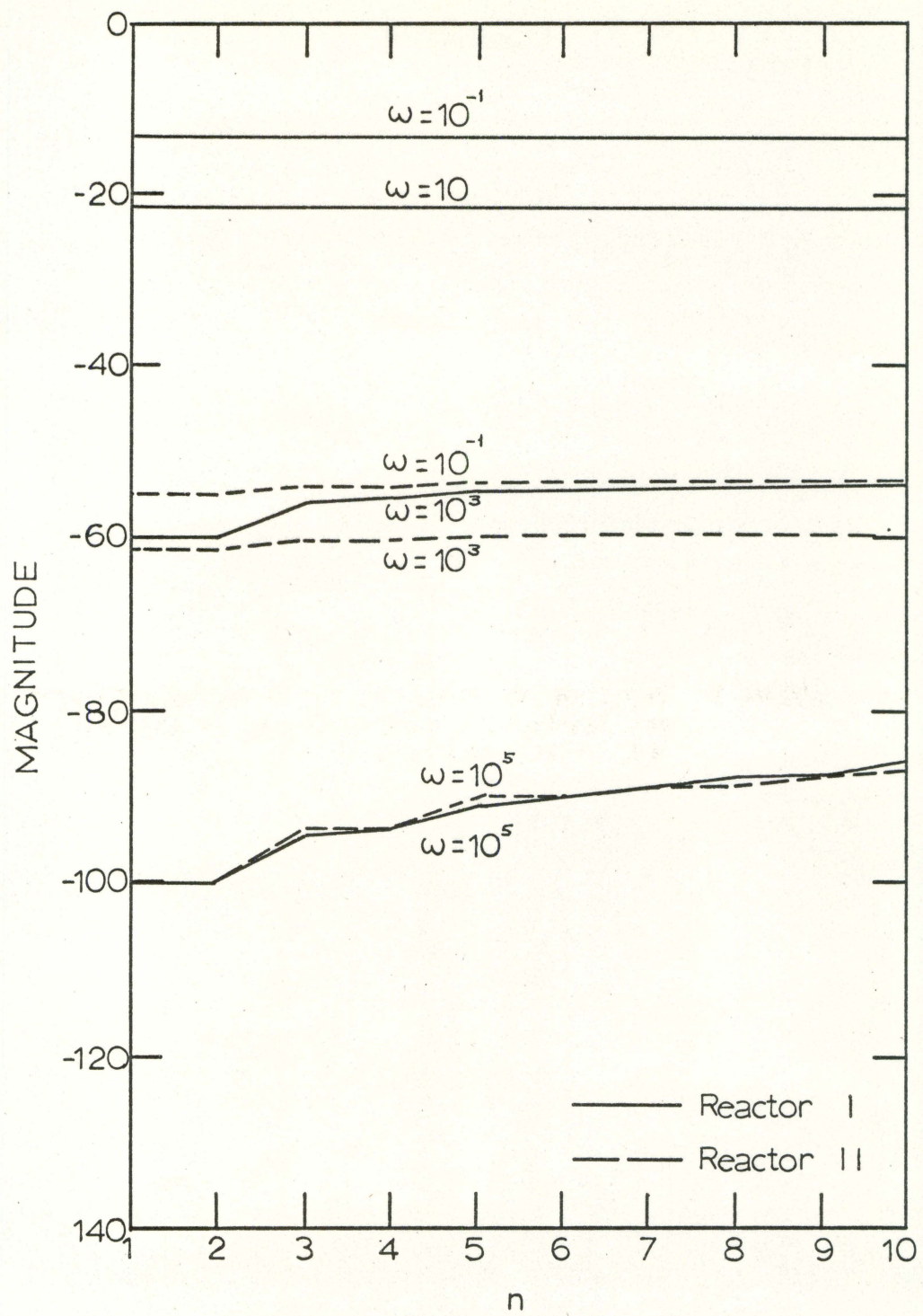


Figure 5. Phase shift vs number of terms for Reactor I and Reactor II, same positions of absorber and neutron detector

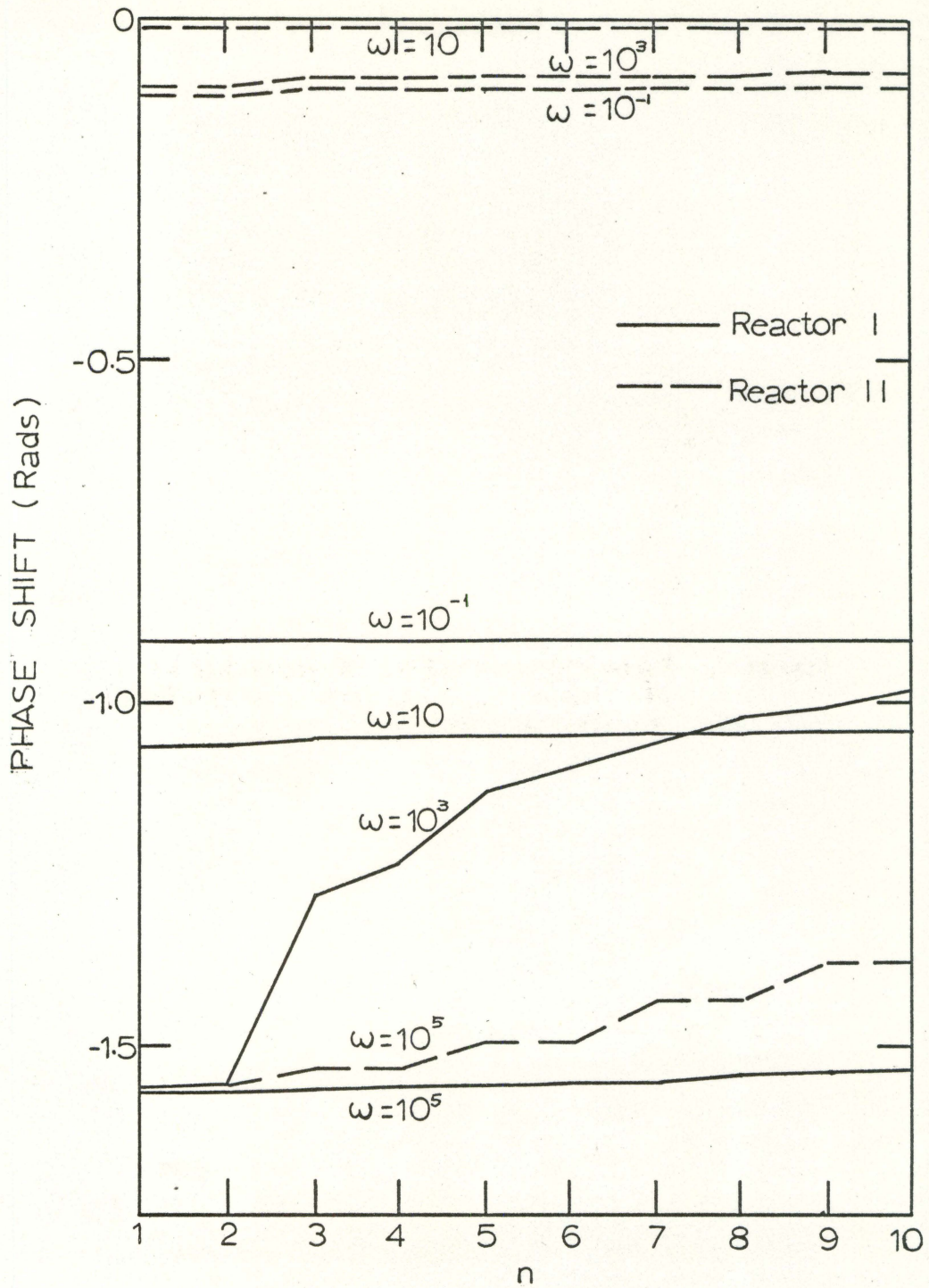


Figure 6. Magnitude vs frequency for Reactor I

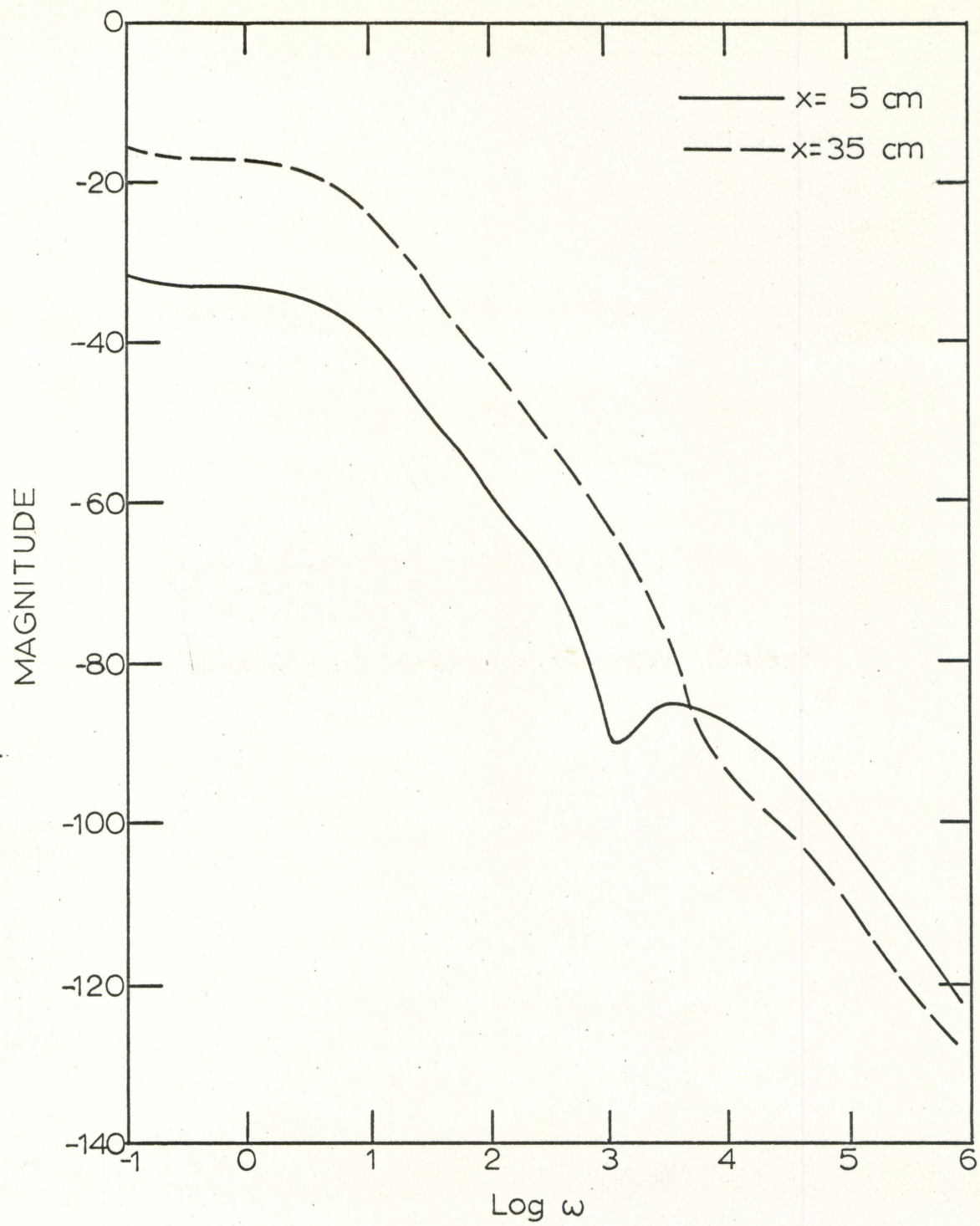


Figure 7. Phase shift vs frequency for Reactor I

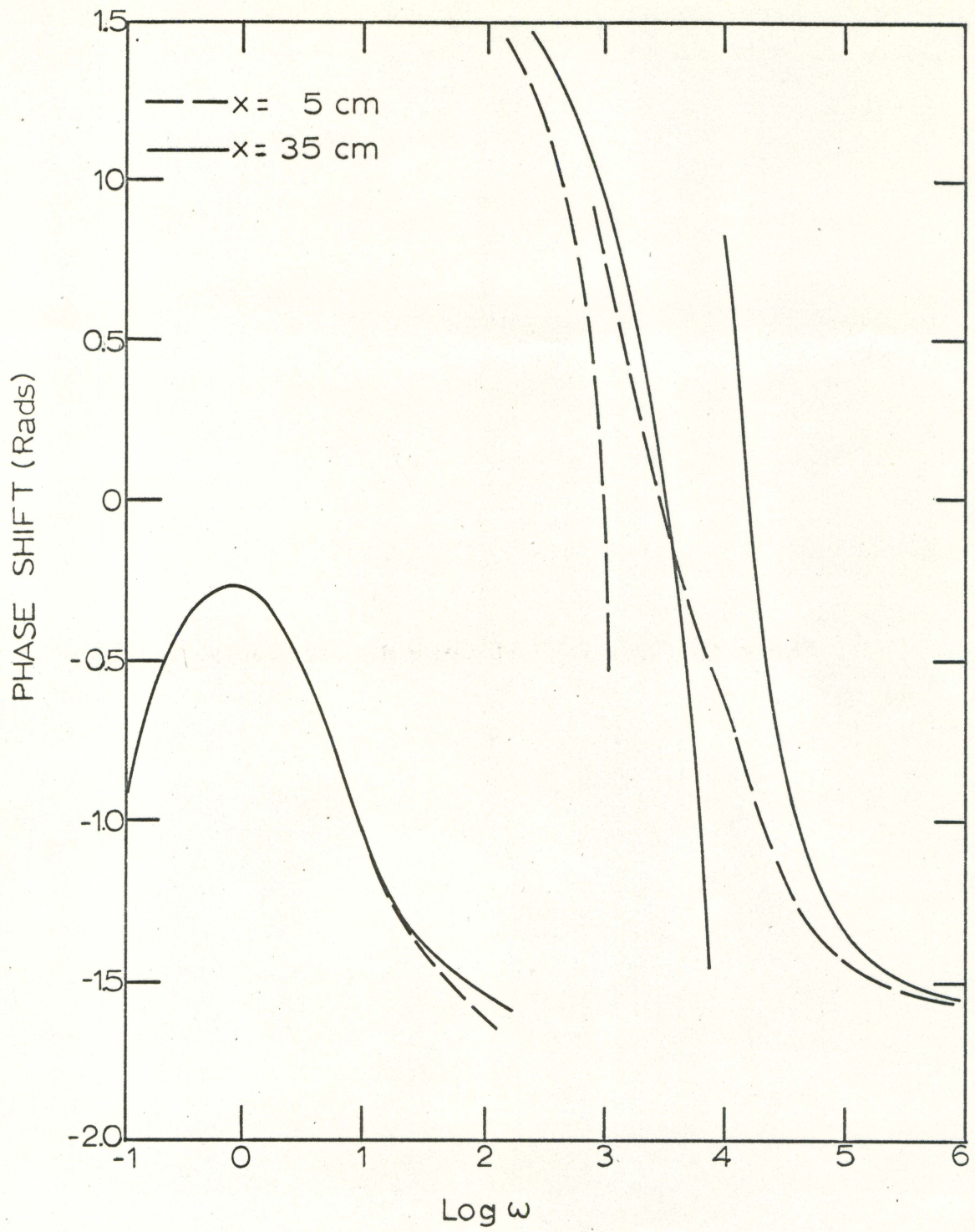


Figure 8. Magnitude vs frequency for Reactor II

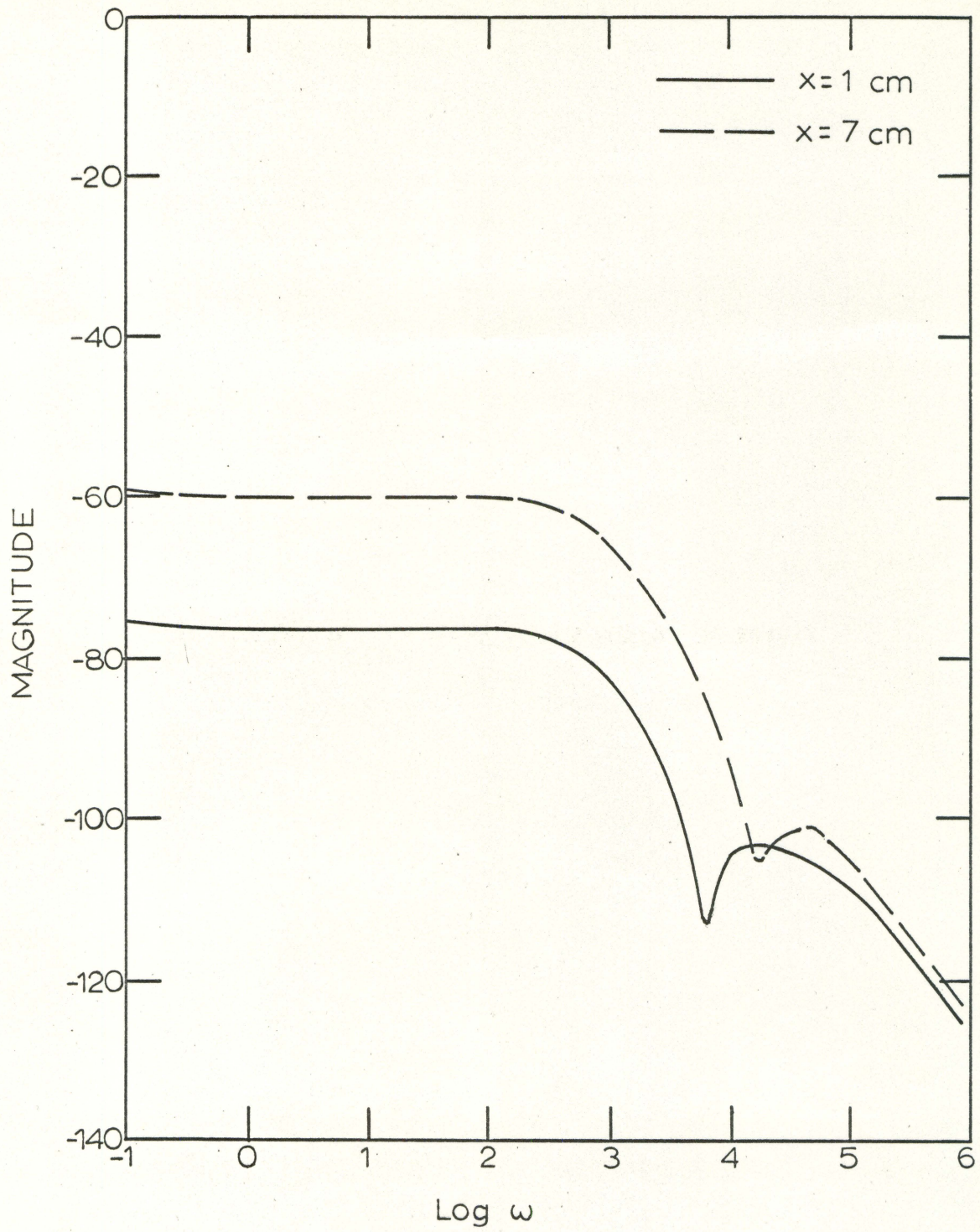


Figure 9. Phase shift vs frequency for Reactor II

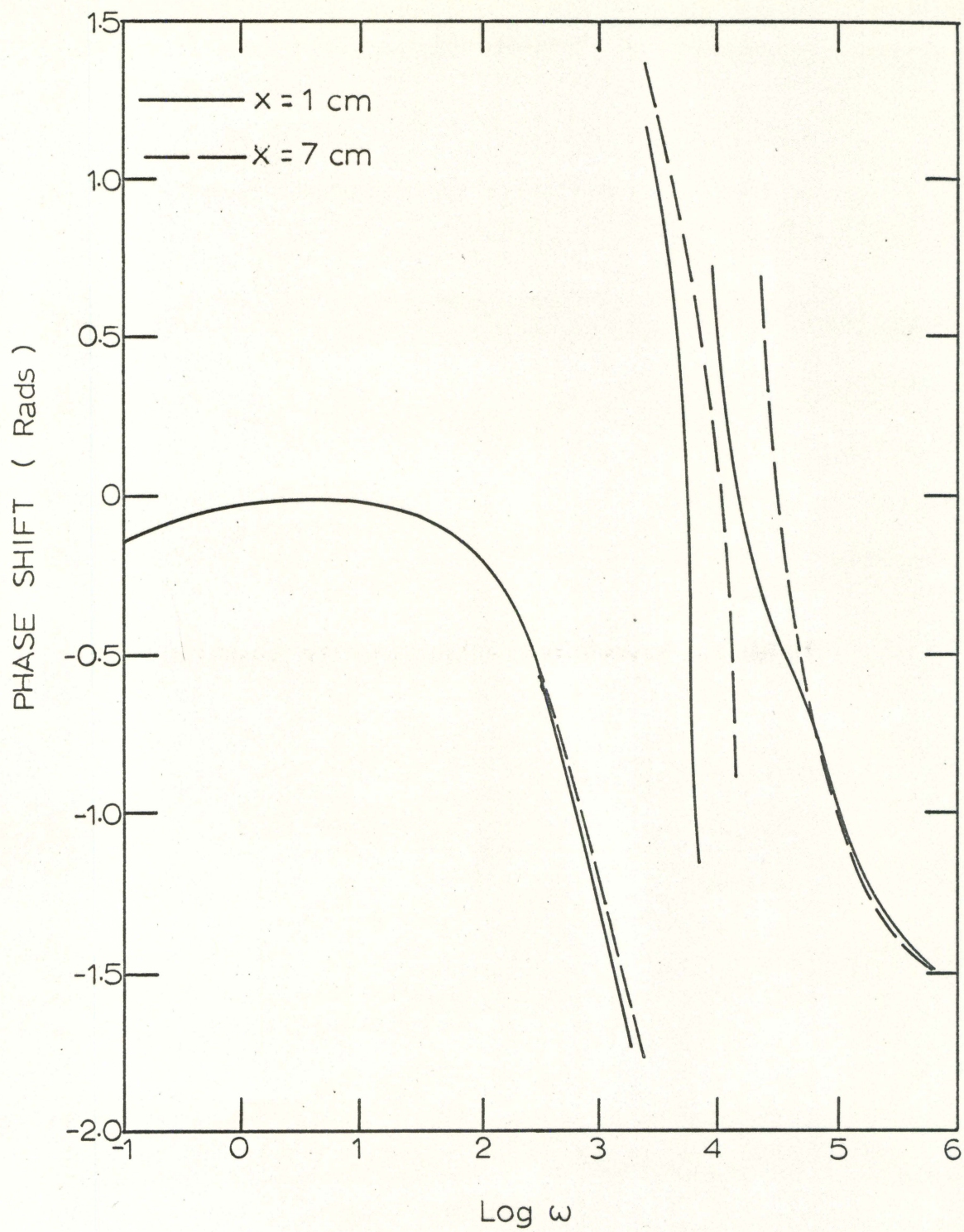


Figure 10. Magnitude vs number of terms for Reactor I

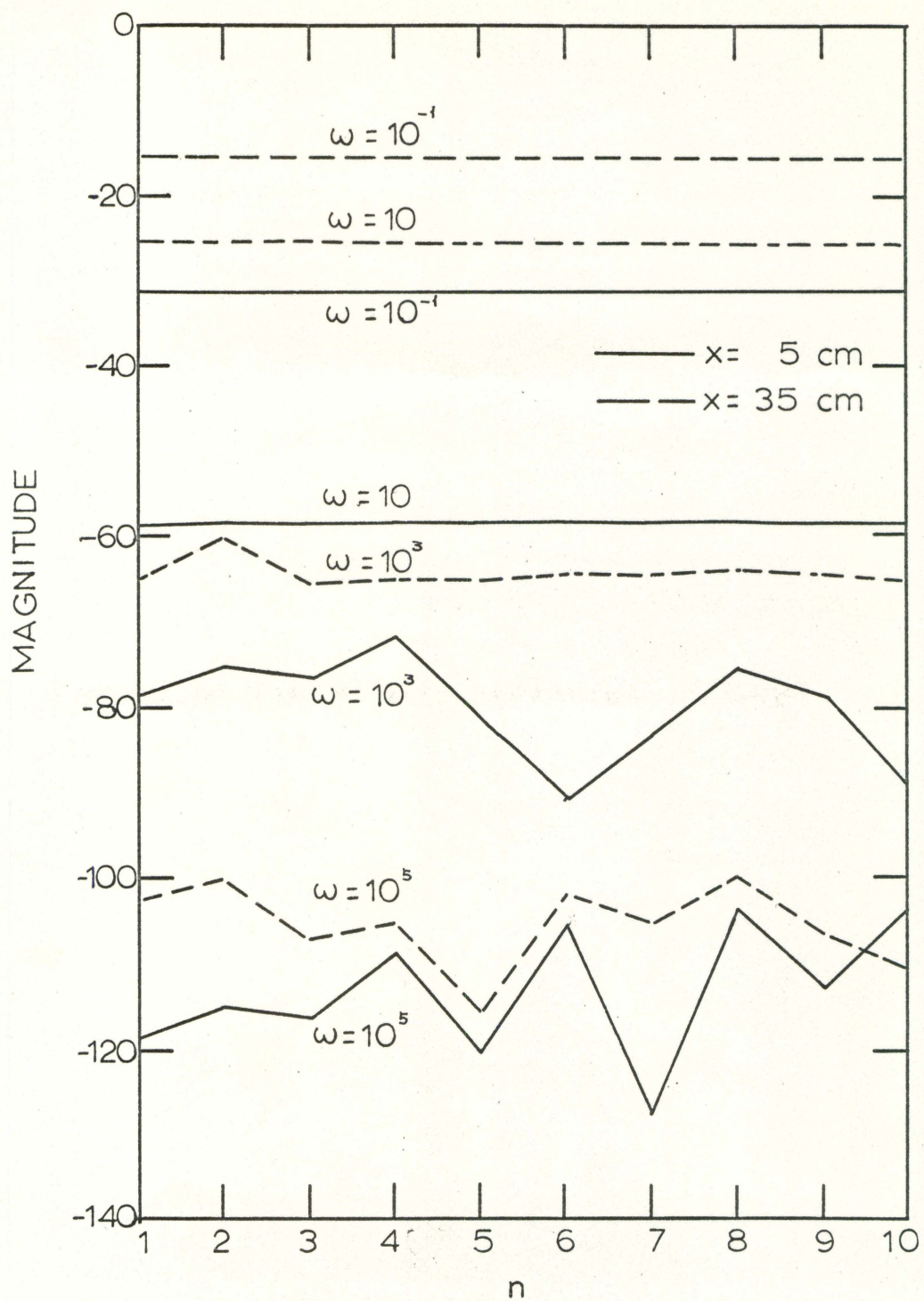


Figure 11. Phase shift vs number of terms for Reactor I

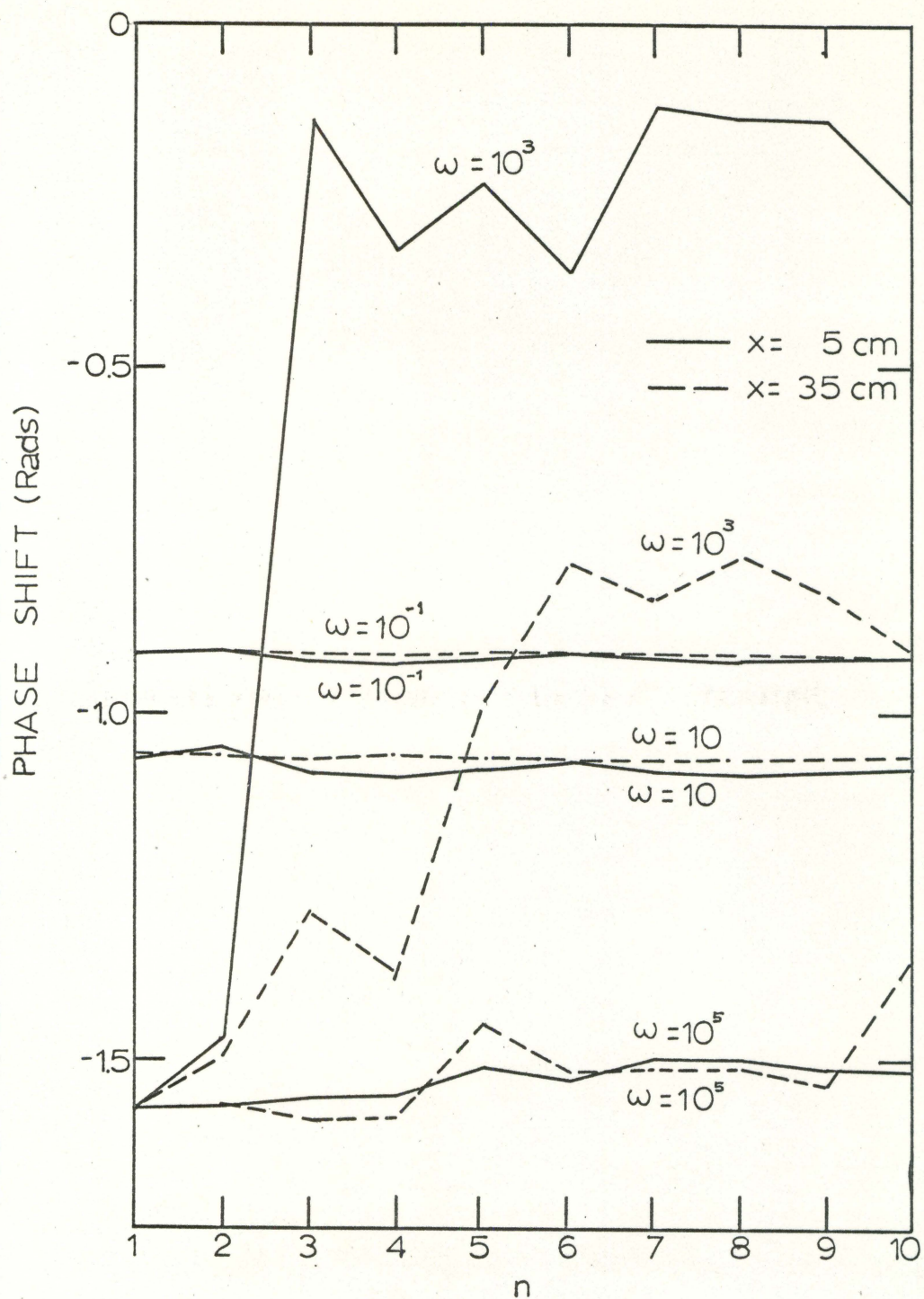


Figure 12. Magnitude vs number of terms for Reactor II

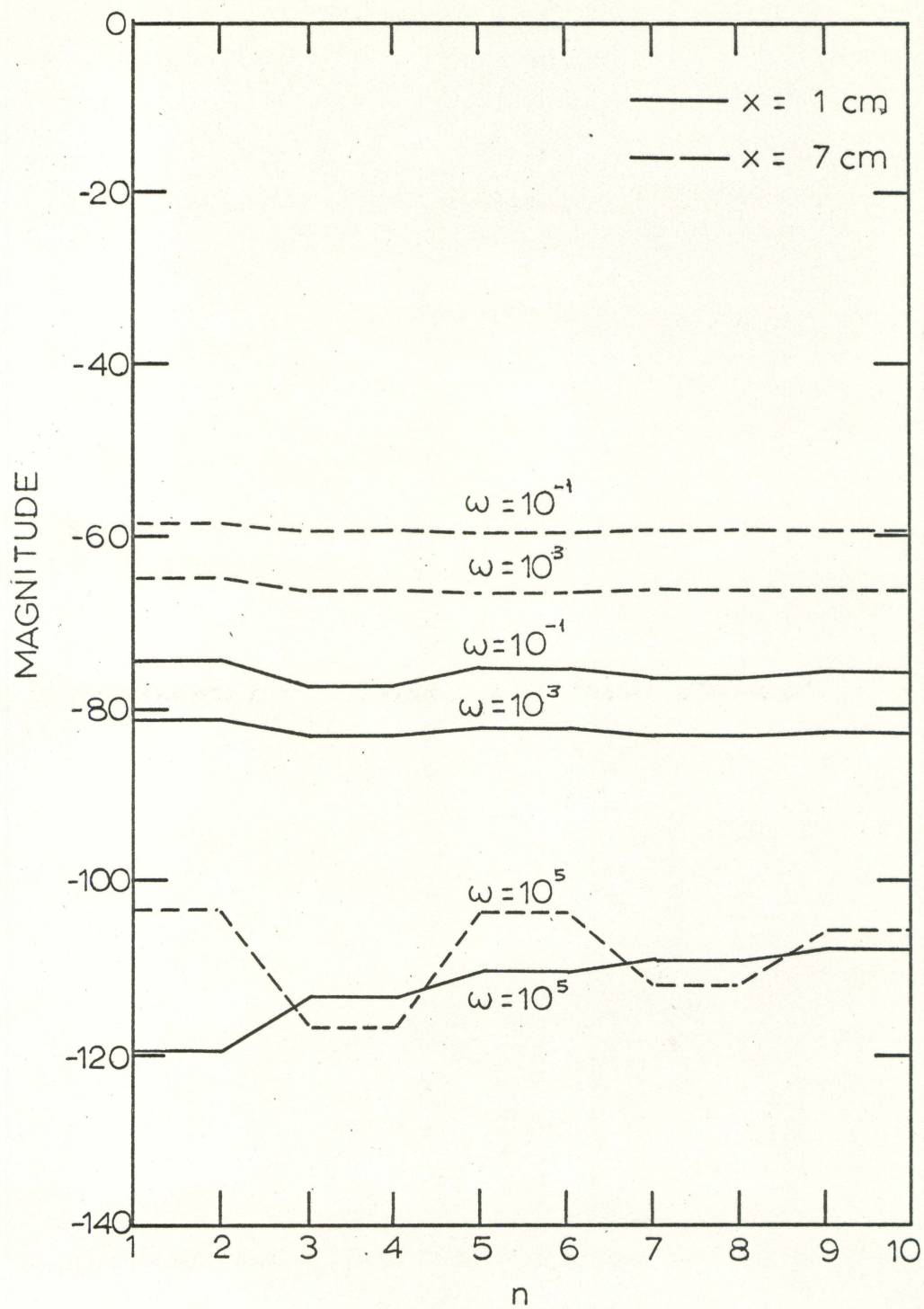
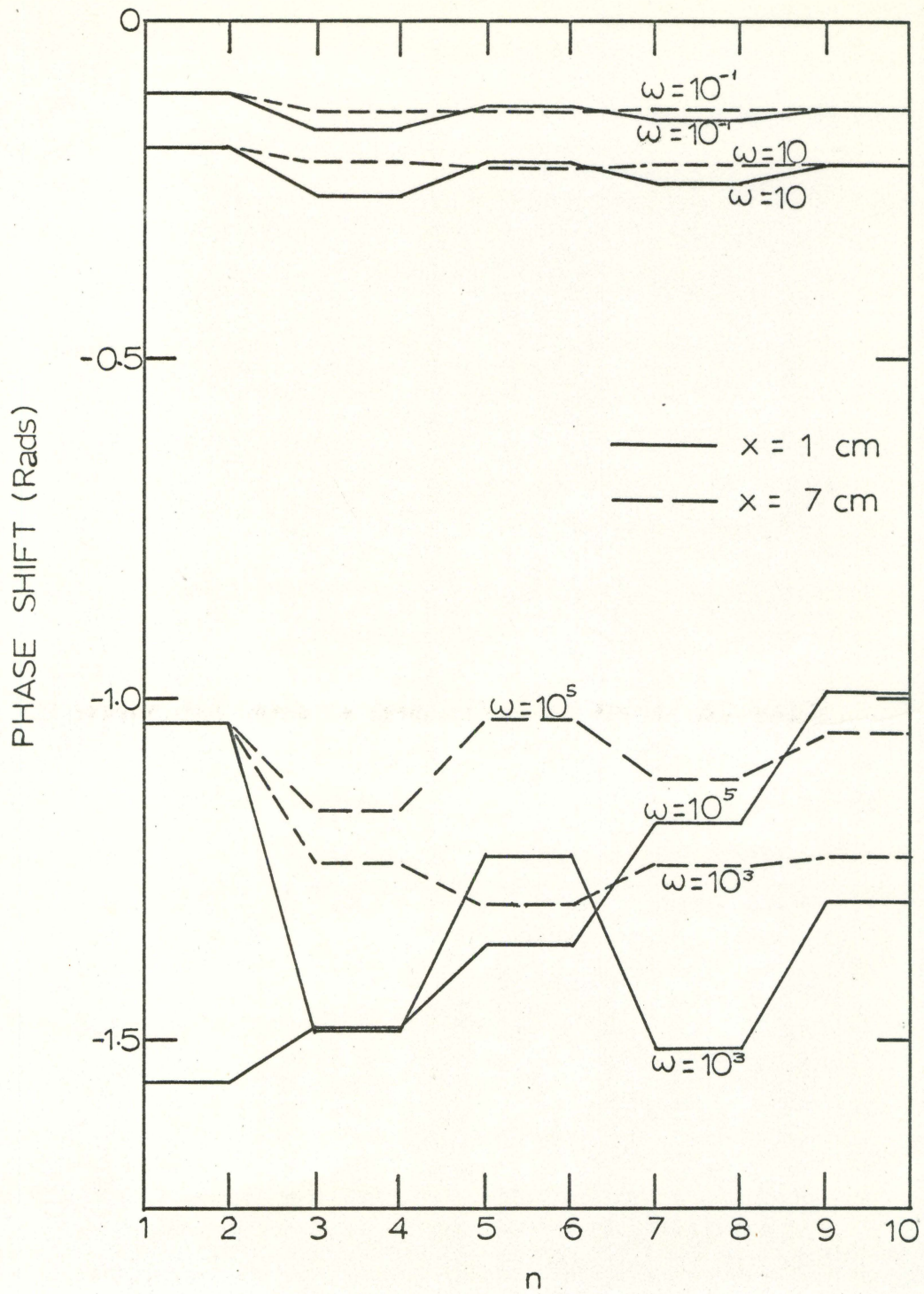


Figure 13. Phase shift vs number of terms for Reactor II



V. DISCUSSIONS

A. On the Theory

In obtaining the spatial dependent transfer function, many assumptions were made. In this section, these assumptions are discussed.

Since the diffusion equations can not be valid without the assumption of the homogeneity of the medium, this assumption will not be discussed in detail. However, as for the magnitude of the transfer function, a proportional factor due to the microscopic neutron flux distribution in the unit cell ----- this factor may have a concept similar to that of the hot spot factors in the heat transfer calculations in the core ----- can be considered.

One group assumption of the neutron energy

The eigen function expansion method can be applied to the multigroup diffusion equations under the assumption that the extrapolation distances are the same for all energy neutron groups of neutron flux, i.e., the neutron fluxes of all energy groups satisfy the same boundary condition. Without this additional assumption, the eigen values are different for each energy group. Therefore the orthogonality of the eigen functions can not be used for expressing the neutron source term of each diffusion equation in simple form, because the source terms always contain the neutron flux of another energy group. This assumption for the boundary condition does not seem to cause serious error in the calculation, because the extrapolation distance is defined by

$$d = 0.71\lambda_t = \frac{0.71}{\Sigma_s (1 - \bar{\nu}_0)}$$

in the diffusion theory and the scattering cross section, Σ_s , and the average cosine of the scattering angle per collision, $\bar{\mu}_0$, are not strongly dependent of the neutron energy. However, from the point of view that diffusion theory does not give a sufficiently accurate description of the flux distribution near the boundary, as indicated by Weinberg and Wigner (20), the multigroup diffusion equations also are not expected to give accurate information near the boundary.

Reflector

In deriving the spatial dependent transfer function, the reactor was assumed to be bare. In the case of a reflected reactor, the neutron flux may be expanded into two series of different eigen functions inside and outside of the core. Therefore, the transfer function may be of a more complicated form. It is, however, interesting to check the effect of the reflector on the transfer function, especially of those reactors which have large reflector savings and a large peaking of the thermal neutron flux, such as the Material Testing Reactor. In these reactors, the reflection of neutrons by the reflector is quite significant.

In connection with the multigroup treatment of the diffusion equation, it seems nearly impossible to expand the neutron fluxes of all energy groups into infinite series, for the existence of the reflector results in large differences in the boundary conditions for each energy group.

Precursor concentration

The precursor concentrations were assumed to satisfy the same boundary condition as that of the neutron flux. Actually, they do not exist outside of the effective core, while their distributions are proportional to the neutron flux distribution inside of the effective core. However,

since the precursor concentrations appear as neutron sources in the diffusion equation and the diffusion of the produced neutron during the slowing down is not considered in this equation, this assumption may not cause as much error in the calculation as expected.

When diffusion during the slowing down of the neutron is taken into consideration, it is necessary to assume the neutron sources including the delayed neutron sources satisfy the same boundary condition as that of the neutron flux. Then, the neutron source terms become the products of the neutron flux and the weighing factors. These weighing factors are the three dimensional Fourier transforms of the slowing down kernels and are functions of the eigen values. This method was discussed in the article of Weinberg and Schweinler (19).

Telegrapher's equation

The first approximation of the transport equation, P-1 approximation, yields the Telegrapher's equation

$$\frac{3D}{v^2} \frac{\partial^2 \phi}{\partial t^2} + \frac{1}{v} (1 - 3DE_a) \frac{\partial \phi}{\partial t} = DV^2 \phi - \Sigma_a \phi + S.$$

The diffusion equation, Equation 1, is obtained for the case of a sufficiently large average neutron velocity, v . The Telegrapher's equation can be solved by the method discussed in III. The solution of the Telegrapher's equation contains an s^3 term in the denominator. Therefore, the effect of this term will be apparent in the high frequency region. The coefficient of the additional term, however, is smaller than that of the first derivative term in the diffusion equation by a factor of approximately $10^{-5} \sim 10^{-6}$, because the average neutron velocity is usually larger than 2.2×10^5 cm/sec. Therefore, the effect of this term will be

important for frequencies above 10^5 rad/sec. According to the calculation of Loewe (15), the curves of the magnitude and the phase shift of the solution of the Telegrapher's equation separate from that of the usual diffusion equation at about 10^4 rad/sec and show a different tendency.

B. On the Results of the Numerical Calculation

Figure 2 shows the magnitude, $|G|$, of the transfer function of Reactor I and Reactor II, when the neutron flux fluctuation is observed at the same place of the absorber. The resultant curves are quite different from the transfer function for the space-independent case in the high frequency region. The space-independent transfer function, $(s + \lambda)/s(s + \beta/l^2)$, indicates that the break frequency of the magnitude are $\omega_1 = \lambda$ and $\omega_2 = \beta/l^2$. Since the effective neutron lifetimes of Reactor I and Reactor II are

$$\frac{1}{(1 + L^2 B^2) v \Sigma_a} = 9.77 \times 10^{-4}, 4.76 \times 10^{-5} \text{ sec,}$$

respectively, the break frequencies in the high frequency region are 6.55 and 134 rad/sec, respectively. For Reactor I, the magnitude curve shows that the break frequency is approximately 6.0 rad/sec and the difference between these values is approximately 9%. In the case of Reactor II, it is found that the fitting of an asymptote to the curve is difficult, and the inspection of the curve indicates that the break frequency is larger by about ten times than the calculated value from the neutron lifetime. When these results are compared with that of the magnitude curves of different positions of the observation, each curve gives different value of the break frequency. This difference is not so large for the weak

absorbing medium, such as Reactor I. Since the lifetime of neutron is defined by $1/v\ell_a$, the hardening of neutron flux does not affect the lifetime. Therefore, this difference may be considered to be a result of the space-dependency of the transfer function. From this point of view, the measurement of the neutron lifetime, ℓ^* , or the fraction of delayed neutrons, β , by the pile oscillator technique may introduce serious error. However, Loewe (14) shows that when the position of the observation is far from the position of the absorber, the break frequency obtained by experiment appears to be reasonably good. It seems that the break frequency gradually decreases with increasing distance between the observation and the absorber. The space-dependency of the transfer function manifests itself more clearly in the phase shift curve. Figure 3 shows that at high frequencies, above 100 rad/sec for Reactor I and 1000 rad/sec for Reactor II, the second peaking appears, while the phase shift was supposed to be nearly $-\pi/2$ from the one point model theory. This resonance will be due to the resonance of the original wave produced by the oscillation of the absorber and the reflected neutron wave. The presence of resonance is expected from the fact that the solution of the equation is similar to the propagating wave in a damping medium. In the usual theory of the wave propagation, it is a well known fact that the resonance is produced by the reflection of the wave from the boundary. In other words, the neutron which is produced at a certain instance travels through the medium and is absorbed at some other place after the time of ℓ^* from its birth. The absorption of this neutron produces newly born neutrons and this new neutron affects the neutron flux at the birth place of the old neutron after a time on the order of $2\ell^*$. The total

time elapsed from the birth of the old neutron to the arrival of the new neutron is $2 \times l^*$, and this new neutron arrives with the phase lag

$$\Delta\theta = - (2l^*/T) \times 2\pi = - 2l^*\omega, \text{ where } T \text{ is the period of the oscillation.}$$

The most effective mode of the newly born neutron is that with the phase shift of

$$\Delta\theta = -(\text{phase shift}_{\text{uniform absorber}} - \text{phase shift}_{\text{localized absorber}} + 2\pi),$$

i.e., the first mode. At the peak of the resonance, the difference between the phase shift of a localized absorber and that of a uniform one is approximately 0.38 rad. for both cases. Therefore, the total phase lag is approximately 3.42 radians and the frequencies where the peakings appear are calculated as $\omega = \Delta\theta/2l^* = 1.75 \times 10^3$, and 3.6×10^4 for Reactor I and Reactor II, respectively. These values are consistent with the calculated values.

Figure 4 and Figure 5 show the calculated magnitude and the phase shift with the truncated series up to ten terms. As seen in these figures, the convergence speed of the series is quite satisfactory at the low frequency region, but at the high frequency region both of the magnitude and the phase shift do not converge fast and it can not be concluded that ten terms are sufficient for this calculation.

Figure 6 and Figure 7 show the magnitude and the phase shift of Reactor I when the neutron is observed at different positions from that of oscillating absorber. Although the magnitudes of the transfer functions show dips at approximately $10^3 \sim 10^4$ rad/sec, it is considered that these deviations are due to the poor convergence speed of the series. This fact is shown clearly by Figure 10. In Figure 11, the values of phase shift which is calculated by the truncated series with a number of

terms up to ten. The phase shift shows poorer convergence speed than the magnitude. Figure 8, Figure 9, Figure 12 and Figure 13 show the magnitude, phase shift and convergence speed in the case of Reactor II. These figures show that the distance between the absorber and the detector affect the convergence speed of the series and the larger distance seems to require more terms.

VI. CONCLUSIONS

The spatial dependent transfer function of nuclear reactors are derived theoretically for various geometries with the aid of the eigen function expansion method. As for the numerical example, the transfer functions of two reactors of slab geometry, one of which has a core composition of weak absorption and one which consists of a strong absorbing medium, are calculated using the CYCLONE computer. Conclusions drawn from this investigation are as follows:

1. The transfer function can be derived by a formal calculation procedure by defining the integral transformation with a kernel of an eigen function of the Helmholtz equation.
2. The coefficients of the expansion have the same form as the spatial independent transfer function except the buckling is replaced with the eigen values of the Helmholtz equation.
3. The spatial independent transfer function corresponds to the first term of the series expansion.
4. The results include the importance function of the position. Therefore, it is not necessary to convert the absorption cross section change into an equivalent reactivity change in the calculation.
5. The transfer function to other inputs such as a change of the reactivity or the external neutron source can be derived with the same procedure.
6. The spatial dependent transfer function has a different magnitude and phase shift at high frequencies from that of the spatial independent transfer function. This difference is due

to the resonance of the neutron waves in the propagating medium.

7. The measured break frequency is not accurate when the pile oscillator and the neutron detector are located near each other. Therefore, the neutron flux change for the measurement of the neutron lifetime or the fraction of delayed neutrons should be measured with the detector located far from the pile oscillator.
8. The deviations of the magnitude and the phase shift from the one point model become more significant for a strong absorbing medium.
9. The convergence speed is comparatively fast when the neutron detector is located near the oscillating absorber. However, the speed of convergence is very slow at high frequencies, when the neutron detector and the absorber are located far apart. A large number of terms are necessary to obtain satisfactory values of the phase shift in such cases.

VII. SUGGESTIONS FOR FURTHER STUDY

A. On the Theory

In the section of the Discussion, Part A., the development of this theory to the more generalized cases was discussed. It was pointed out that further intensive investigations are necessary in order to generalize the theory.

It is clear that the transfer function can be derived for other inputs such as changes in the multiplication factor or in an external neutron source.

It should be pointed out that the problem of the convergence of the series needs further investigation.

As for the applications of this technique, it can be applied to the stability analysis of boiling water reactors with a void coefficient feedback. It is well known that the reactivity introduction into the core due to the formation of steam bubbles is not spatially independent ---- usually it is treated as a homogeneous distribution over the core because of the difficulty of theoretical treatment ---- but is basically proportional to the power density distribution in the core. This problem can be treated with the same technique as that for the localized point absorber. The multiplication factor is to be defined as a function of position, while it is originally defined as a characteristic of the whole core system. The multiplication factor defined in this fashion means that when the system is filled with the local medium with the multiplication factor, $k_{\infty}(\vec{r})$, the system multiplication factor will be $k_{\infty}(\vec{r})$ as a whole. Then the distribution of the multiplication factor is proportional to the

neutron flux distribution, because the void formation is proportional to the neutron flux distribution and the reactivity induced is also proportional to the void fraction. Besides the diffusion equation and the precursor equation, the heat transfer equation which describes the relation between the neutron flux and the heat transferred to the coolant is necessary. The heat transfer equation introduces a new time constant due to the transfer delay of heat from the fuel to the coolant. By analyzing this set of equations and using techniques of control theory, it can be determined if an unstable spatial oscillation can exist or not, or what kind of oscillation can exist.

The problem of Xenon oscillations in the core can be analyzed in a similar fashion.

As for the simulation of the spatial dependent transfer function, the method of Hanson and Foulke (7), in which the core is divided into several regions and the diffusion equation and the precursor equation of each region are simulated with an analogue circuit, will be satisfactory, if the number of amplifiers are restricted to a reasonable number so that serious error is not introduced.

B. On the Experiment

In this investigation, the results of the calculations are not compared with experimental data, because a suitable pile oscillator was not available. In this section, some thought is presented on how these theoretical results could be experimentally verified, included are some specific comments on the redesign of the present pile oscillator.

Revolution speed

As shown in the results of the calculations, the difference between the spatial dependent transfer function and the spatial independent transfer function becomes significant at frequencies above approximately 10^2 rad/sec. It is desirable that the frequency range of the pile oscillator covers the frequency range of the second peaking in the phase shift curve of the spatial dependent transfer function. From this point of view, the desirable maximum frequency of the oscillating absorber is 10^4 rad/sec or more. But this maximum frequency corresponds to approximately 96000 rpm, when one rotation of the oscillator rotor corresponds to one cycle of the absorber oscillation, and it is impossible to provide such a high revolution speed. The method in which the oscillation of the absorber is obtained by the vibration on a line presents difficulty in the high frequency region because of the reason described later. In order to reduce the revolution speed, the absorbers on the rotor and the stator should be arranged in such a way that one rotation of the rotor corresponds to more than one cycle of the absorber oscillation. This can be accomplished by dividing the peripheries of the rotor and the stator into 8 or 16 equal sections and attaching the appropriate absorber patterns to each section. This arrangement will require a high accuracy of fabrication of the rotor and the stator. Even if such an assembly can be fabricated with satisfactory accuracy, the maximum input frequency will be limited to 6.0×10^3 rad/sec, when the shaft of the rotor is connected directly to the shaft of a 6-pole induction motor. It is not desirable to amplify the speed of the rotor more than that of the motor, since the probability of an accident and failure of the equipment is increased at

higher speed. Although the speed of 3600 rpm is not so severe in the engineering sense, the shaft system, including the arrangement of bearings, should be designed with utmost care in order to avoid undesirable vibration of the equipment and an unexpected accident.

Speed control and measurement

Since the present equipment has a revolution speed range of 3.1 to 1500 rpm and the speed of the motor is reduced with gears, the driving system including the speed control system will be satisfactory when the shaft of the motor is directly connected to that of the motor. The position indicator of the rotor should be replaced with a more accurate sensing device, such as a position detector using a phototube, because an error in the measurement of the rotor position is amplified 16 times in the phase shift measurement.

Safety circuit

As seen in the results of the calculations, the magnitude of the transfer function is quite small in the high frequency region. Therefore, a large amplitude of the absorber oscillation is required for an accurate measurement of the transfer function. When a linear oscillation of the absorber is used for the input, the amplitude of the oscillation must be very large. A large linear movement of the absorber at high frequency means increased complexity of fabrication and control of the equipment over that of the rotating machine. For this reason, this method is not recommended. Due to the requirement of the magnitude measurement, it is desirable to use the maximum value of the available excess reactivity in the amplitude of the oscillation. If the speed of the rotor should suddenly drop to a lower speed by some accident, it would result in a large

reactivity insertion to the core. To prevent such an accident it is necessary to provide a safety circuit to shut down the reactor in case the speed should drop to some limiting value.

Method of measurement

Simple calculation shows that the fluctuation of neutron density due to the oscillating absorber becomes comparable to the fluctuation due to the statistical error of the measurement at frequencies higher than 100 rad/sec. Therefore, at such high frequencies the direct analysis of the neutron density fluctuation is not possible. The neutron density fluctuation and the relative position of the rotor and the stator must be recorded by some electronic device of fast response. The recorded data must be analyzed by cross correlation techniques, otherwise it is impossible to separate the fluctuation of the neutron density due to the oscillation of the absorber from the statistical fluctuation of the neutron density.

VIII. NOMENCLATURE

a	: dimension of core in x-direction	cm
$A_{\vec{n}}$: coefficient of series with the suffix vector \vec{n}	
b	: dimension of core in y-direction	cm
B^2	: buckling of core	cm^{-2}
$B_{\vec{n}}$: eigen value of the Helmholtz equation with the suffix vector \vec{n}	
c	: dimension of core in z-direction	cm
C_i	: concentration of the i th group of delayed neutron precursors	n/cm^3
d	: extrapolation distance	cm
D	: diffusion coefficient	cm
f	: thermal utilization	
G	: transfer function of reactor	
$j_{l,m}$: m th zero of the l th order or the $l + \frac{1}{2}$ th order Bessel function	
k_{∞}	: multiplication factor of infinite medium	
L	: diffusion length	cm
p	: resonance escape probability	
q	: non leakage factor of neutrons during slowing down process	
\vec{r}	: vector of position	
R	: radius of core	cm
s	: complex variable	
S	: external neutron source	$\text{n/cm}^3 \cdot \text{sec}$

t	: time	sec
v	: average velocity of thermal neutrons	cm/sec
X_i	: integral transformed concentration of the i^{th} group of delayed neutrons	
a	: vector of position of localized absorber	
β	: total fraction of delayed neutrons	
β_i	: fraction of the i^{th} group of delayed neutrons	
δ	: Dirac's delta function	
ϵ	: fast fission factor	
η	: average number of neutrons produced per neutron absorbed	
λ	: decay constant of average group of delayed neutron precursors	sec ⁻¹
λ_i	: decay constant of the i^{th} group of delayed neutron precursors	sec ⁻¹
$\bar{\mu}_0$: average cosine of scattering angle per collision	
ν	: average number of neutrons released per fission	
Σ	: macroscopic cross section	cm ⁻¹
$\Delta\Sigma_a$: amplitude of absorption cross section change by localized absorber	cm ⁻¹
τ	: Fermi age	cm ²
ϕ	: neutron flux	n/cm ² sec
ϕ	: Laplace transformed neutron flux	

$\psi_{\vec{n}}$: eigen function with suffix vector \vec{n} of the Helmholtz equation

ψ : integral transformed neutron flux

ω : frequency of oscillation

rad/sec

∇^2 : Laplacian

Subscripts

a : absorption

a,f : absorption of fuel

i : ith part

r : r-direction

s : scattering

u : unsteady state

x : x-direction

y : y-direction

z : z-direction

IX. BIBLIOGRAPHY

1. Akcasu, Z. General solution of the reactor kinetics equations without feedback. Nuclear Science and Engineering 3: 456-467. 1958.
2. Brownell, A. Advanced mathematics in physics and engineering. New York, N.Y., McGraw Hill. 1953.
3. Dougherty, D. E. and Shen, C. H. The space time neutron kinetic equations obtained by the semi direct variational method. Nuclear Science and Engineering 13: 141-148. 1962.
4. Franz, J. P. Pile transfer function. U.S. Atomic Energy Commission Report AECD-3260. [Technical Information Service Extension, AEC]. 1949.
5. Garabedian, H. L. and Foderaro, A. Two group reactor kinetics. Nuclear Science and Engineering 14: 22-29. 1962.
6. Habetler, G. J. and Martino, M. A. Eigenfunction expansions associated with the multigroup diffusion model. American Nuclear Society Transactions 1: 27-28. 1958.
7. Hanson, P. T. and Foulke, L. R. Investigations in spatial reactor kinetics. Nuclear Science and Engineering 17: 528-533. 1963.
8. Harre, J. M. Nuclear reactor control engineering. New York, N.Y., D. Van Nostrand. 1963.
9. Hayashi, S., Hoshino, T. and Wakabayashi, J. Nuclear reactor spatial kinetics expressed in the transfer function form. Japan Nuclear Society Journal 5: 503-507. 1963.
10. Ishikawa, H., Asaoka, T. and Sasakura, Y. Design calculations of JRR-3 (Natural uranium heavy-water research reactor). Part 1. Core calculations. Japan Atomic Energy Research Institute Report JAERI-1001. [Japan Atomic Energy Research Institute, Tokyo]. 1959.
11. Kaplan, S. The properties of finality and the analysis of problems in reactor space-time kinetics by various expansions. Nuclear Science and Engineering 9: 357-361. 1961.
12. Keppin, G. R. and Wimet, T. F. Reactor kinetic functions; A new evaluation. Nucleonics 16: 86-90. October 1958.
13. Lewins, J. The approximate separation of kinetic problems into time and space function by a variational principle. Reactor Science 12: 108-112. 1960.

14. Loewe, W. E. Space dependent effects in the response of a nuclear reactor to forced oscillations. Unpublished paper. Chicago, Illinois, Illinois Institute of Technology. 1964.
15. Loewe, W. E. Space-dependent transfer function. American Nuclear Society Transactions 6: 215-216. 1963.
16. Moriguchi, S., Utagawa, K. and Hitotsumatsu, S. Sugaku koshiki, III Tokushu kansu. (Mathematical Formulas, III Special functions. Translated title) Tokyo, Iwanami. 1960.
17. Nordheim, L. W. Pile kinetics. U.S. Atomic Energy Commission Report MDDC-35. [Manhattan District, Oak Ridge, Tenn.]. 1946.
18. Schultz, M. A. Control of nuclear reactors and power plants. 2nd ed. New York, N.Y., McGraw-Hill. 1961.
19. Weinberg, A. M. and Schweinler, H. C. Theory of oscillating absorber in a chain reactor. Physical Review 74: 851-863. 1948.
20. Weinberg, A. M. and Wigner, E. P. The physical theory of neutron chain reactors. Chicago, Illinois, The University of Chicago Press. 1958.

X. ACKNOWLEDGMENTS

The author wishes to express his sincere appreciation to Dr. Richard A. Danofsky for his tireless counsel and instructive advice during both the investigation and the course work.

The author wishes to thank Dr. Glenn Murphy for his kind guidance and encouragement given to the author during the course of study.

The acknowledgment is extended to Dr. Jerald C. Mathews for his helpful advice and inspection of the theory.

Many thanks are also due to both staffs of Nuclear Engineering Department and the CYCLOSE Computer Laboratory for their advice and assistance.

XI. APPENDIX

Table 2. Calculated data for Reactor I and Reactor II
 $\alpha=x=60$ cm for Reactor I, $\alpha=x=15$ cm for Reactor II
 $n=10$

Frequencies rad/sec	Reactor I		Reactor II	
	$ G $	$\angle G$	$ G $	$\angle G$
1.0×10^{-1}	-13.189	-0.91030	-53.490	-0.10300
1.6	14.212	.62803	53.810	.080637
2.5	14.698	.44060	53.977	.057240
4.0	14.944	.31744	54.062	.036950
6.4	15.060	.26991	54.093	.024621
1.0×10^0	-15.174	-.27482	-54.106	-0.016727
1.6	15.390	.33641	54.112	.011908
2.5	15.838	.45250	54.114	.0097841
4.0	16.829	.63363	54.115	.0096776
6.4	18.651	.85075	54.116	.011746
1.0×10^1	-21.227	-1.0467	-54.117	-0.016141
1.6	24.611	1.2055	54.119	.024326
2.5	28.181	1.3022	54.123	.037110
4.0	32.099	1.3527	54.134	.058716
6.4	36.044	1.3574	54.164	.093321
1.0×10^2	-39.710	-1.3223	-54.233	-0.14468
1.6	43.340	1.2465	54.409	.22762
2.5	46.391	1.1492	54.797	.34290
4.0	49.074	1.0499	55.671	.50423
6.4	51.345	0.99033	57.288	.68296
1.0×10^3	-53.429	-0.98122	-59.539	-0.82340
1.6	55.757	1.0034	62.317	.90318
2.5	58.096	1.0418	64.890	.92080
4.0	60.705	1.1003	67.299	.92315
6.4	63.531	1.1767	69.576	.94690
1.0×10^4	-66.492	-1.2605	-71.831	-0.98917
1.6	69.943	1.3480	74.345	1.0466
2.5	73.494	1.4178	76.890	1.1152
4.0	77.414	1.4719	79.815	1.2013
6.4	81.429	1.5081	83.066	1.2937
1.0×10^5	-85.278	-1.5304	-86.465	-1.3745
1.6	89.349	1.5455	90.291	1.4414
2.5	93.221	1.5546	94.059	1.4861
4.0	97.302	1.5607	98.093	1.5173
6.4	+101.38	1.5645	-102.16	1.5372

Table 3. Convergence tendency of series, A
 $\omega = 1.0 \times 10^{-1}$ rad/sec

Number of terms	Reactor I $a = x = 60$ cm		Reactor II $a = x = 15$ cm	
	$ a $	$\langle G$	$ a $	$\langle G$
1	-13.239	-0.91766	-54.734	-0.11777
2	13.234	.91701	54.734	.11777
3	13.209	.91327	53.959	.10858
4	13.206	.91278	53.959	.10858
5	13.199	.91181	53.698	.10547
6	13.196	.91138	53.698	.10547
7	13.194	.91107	53.568	.10392
8	13.192	.91070	53.568	.10392
9	13.191	.91060	53.491	.10301
10	13.189	.91030	53.491	.10301

Table 4. Convergence tendency of series, B
 $\omega = 1.0 \times 10^2$ rad/sec

Number of terms	Reactor I $a = x = 60$ cm		Reactor II $a = x = 15$ cm	
	$ a $	$\langle G$	$ a $	$\langle G$
1	-40.141	-1.5154	-55.586	-0.16717
2	40.087	1.4993	55.586	.16717
3	39.877	1.40000	54.741	.15318
4	39.850	1.3870	54.741	.15318
5	39.797	1.3616	54.457	.14843
6	39.772	1.3503	54.457	.14843
7	39.755	1.3421	54.317	.14608
8	39.334	1.3325	54.317	.14608
9	39.728	1.3301	54.233	.14468
10	39.710	1.3223	54.233	.14468

Table 5. Convergence tendency of series, C

$$\omega = 1.0 \times 10^5 \text{ rad/sec}$$

Number of terms	Reactor I $a = x = 60 \text{ cm}$		Reactor II $a = x = 15 \text{ cm}$	
	$ G $	$\angle G$	$ G $	$\angle G$
1	-100.126	-1.5707	-99.999	-1.5649
2	99.635	1.5706	99.999	1.5649
3	94.347	1.5668	93.989	1.5387
4	93.420	1.5656	93.989	1.5387
5	91.025	1.5607	90.518	1.4960
6	89.764	1.5571	90.518	1.4960
7	88.663	1.5527	88.152	1.4393
8	87.203	1.5453	88.152	1.4393
9	86.785	1.5425	86.465	1.3745
10	85.278	1.5304	86.465	1.3745